# Gastroenteropancreatic Neuroendocrine Tumors: Role of Imaging in Diagnosis and Management[1]

Dushyant V. Sahani, MD
Pietro A. Bonaffini, MD
Carlos Fernández–Del Castillo, MD
Michael A. Blake, MBBCh

Gastroenteropancreatic neuroendocrine tumors (GEP-NETs) are a heterogeneous group of neoplasms that arise from cells of the diffuse neuroendocrine system and are characterized by a wide spectrum of clinical manifestations. All NETs are potentially malignant but differ in their biologic characteristics and the probability of metastatic disease. The pathologic classification of these tumors relies on their proliferation and differentiation. In the past decades, several nomenclatures have been proposed to stratify neuroendocrine tumors, but the World Health Organization classification is the one that is most widely accepted and used. The diagnosis of neuroendocrine tumor relies on clinical manifestation, laboratory parameters, imaging features, and tissue biomarkers in a biopsy specimen. With improved understanding of the natural history and lesion biology, management of GEP-NETs has also evolved. Although surgery remains the only potentially curative therapy for patients with primary GEP-NETs, other available treatments include chemotherapy, interferon, somatostatin analogs, and targeted therapies. Recent improvements in both morphologic and functional imaging methods have contributed immensely to patient care. Morphologic imaging with contrast agent–enhanced multidetector computed tomography and magnetic resonance imaging is most widely used for initial evaluation and staging of disease in these patients, whereas functional imaging techniques are useful both for detection and prognostic evaluation and can change treatment planning.



**Online CME**
*See www.rsna.org/education/ry_cme.html*

**Learning Objectives:**

After reading the article and taking the test, the reader will be able to:

- Describe the role of morphologic and functional imaging in patients suspected of having neuroendocrine tumors (NETs).
- Specify the main imaging features of NETs.
- Discuss the ways in which imaging findings can influence treatment in patients with NETs.

Accreditation and Designation Statement

The RSNA is accredited by the Accreditation Council for Continuing Medical Education (ACCME) to provide continuing medical education for physicians. The RSNA designates this journal-based CME activity for a maximum of 1.0 *AMA PRA Category 1 Credit*™. Physicans should claim only the credit commensurate with the extent of their participation in the activity.

Disclosure Statement

*The ACCME requires that the RSNA, as an accredited provider of CME, obtain signed disclosure statements from the authors, editors, and reviewers for this activity. For this journal-based CME activity, author disclosures are listed at the end of this article.*

[1] From the Department of Radiology, Division of Abdominal Imaging and Interventional Radiology (D.V.S., M.A.B.), and Department of Surgery (C.F.), Massachusetts General Hospital, Harvard Medical School, 55 Fruit St, White 270, Boston, MA 02114; and Department of Diagnostic Radiology, San Gerardo Hospital, School of Medicine, University of Milano-Bicocca, Monza, Italy (P.A.B.). Received December 13, 2011; revision requested January 16, 2012; revision received April 24; accepted June 8; final version accepted June 29. **Address correspondence to** D.V.S. (e-mail: *dsahani@partners.org*).

Gastroenteropancreatic neuroendocrine tumors (GEP-NETs) are a heterogeneous group of neoplasms that arise from cells of the diffuse neuroendocrine system (1–4). They account for about 1.5% of all gastrointestinal and pancreatic neoplasms (5,6). A substantial increase in their incidence has been reported in the past 4 decades (7), currently estimated at 3.0–5.2 cases per 100 000 persons per year and with a prevalence calculated as 35 cases per 100 000 persons per year (8). There is a slightly higher overall incidence for males (52%) compared with females (48%) (7,8). The majority of cases are sporadic, with an overall median age at diagnosis of 63 years (1,7), but they can sometimes occur in patients with complex tumor susceptibility genetic syndromes (9).

In the past 2 decades, improvements in imaging techniques and the extensive use of endoscopy have led to an increased detection of GEP-NETs (1,4,7). These lesions are also now frequently being detected incidentally on high-resolution imaging studies or at endoscopy performed for other indications (10,11). The tumor distribution in the body varies in different parts of the world. In the United States, the majority of lesions are in the foregut (41%) (7), in Europe they are in the midgut (30%–60%), and in Japan the hindgut (60%) is the commonest tumor site (12). In the gastrointestinal tract, 30% of neuroendocrine tumors (NETs) occur in the ileum (4–6), followed by the rectum (21%–27%) and the appendix (17%–20%). Stomach (6%–9%) and duodenum and jejunum (2%–3%) are other less common sites of disease (4–6,13–15), and the colon is an uncommon location (5,6). Pancreatic NETs account for 7% of all GEP-NETs and for up to 10% of all pancreatic neoplasms (Table 1) (1,4,5,16).

NETs can produce metabolically active hormones and amines, and the clinical manifestation of the lesions can be due to their hypersecretion (4). The more common nonfunctioning tumors frequently manifest as locally advanced disease (ie, bowel obstruction, mass effect), or with metastases (mainly to the liver) (4,10,11).

Tumor detection, characterization, and staging are essential in the management of GEP-NETs and for treatment planning (10,17,18). Various morphologic and functional imaging studies are now available and can serve specific roles in the care-path of patients with GEP-NETs with their choice being dependent on the clinical indication.

## Essentials

- Improvements in imaging techniques and extensive use of endoscopic approaches in clinical practice have led to increased detection of gastroenteropancreatic neuroendocrine tumors (GEP-NETs), often incidentally.
- The diagnosis and subsequent investigations are dependent on the clinical manifestation and tumor location: In symptomatic patients, levels of serum and urinary neuroendocrine hormones and of tissue neuroendocrine markers are assayed first.
- All neuroendocrine tumors have a malignant potential, but tumor grade and cell differentiation information at histopathologic examination is essential to accurately stratify the patient's risk for metastases and recurrence.
- Morphologic imaging using contrast-enhanced multidetector CT and MR imaging are most widely used in initial evaluation, in monitoring response to treatment and in screening high-risk individuals, while functional imaging techniques (eg, somatostatin receptor scintigraphy) are useful both for detecting tumors and selecting patients for receptor-targeted therapy.
- Complete surgical resection is the preferred and the potentially curative treatment for GEP-NETs and their metastases; however, medical treatment is offered to control disease and symptoms related to hormone hypersecretion.

## Risk Factors and Etiology

For most of GEP-NETs no identifiable risk factor is evident (1). A higher risk has been observed among women, African Americans, Hispanics, and Asians (19). Moreover, some conditions such as hypergastrinemia, preexisting diabetes mellitus, and ulcerative colitis have been associated with these neoplasms (1,5,19,20), but a clear origin remains unknown.

Up to 25% of GEP-NETs are associated with complex genetic syndromes such as MEN-1, or Wermer syndrome, neurofibromatosis type 1 (NF-1 or von Recklinghausen disease), Von Hippel–Lindau disease, and tuberous sclerosis complex) (Table 2) (4–6,9,16,21,22). In these patients, NETs manifest about 15 years earlier than the age typical for sporadic tumors (8,9) In MEN-1, pancreatic NETs are present in 25%–75% of patients (mostly nonfunctioning and gastrinomas) (9) and are the most common cause of death (23,24). On the other hand, NETs in Von Hippel–Lindau disease are typically benign (generally multiple and nonfunctioning) while renal cell carcinoma (RCC) contributes to mortality in > 50% of cases (9,21,25). In NF-1 and tuberous sclerosis complex, NETs (somatostatinomas, gastrinomas, insulinomas) are uncommon (1%) and are not considered a major clinical feature. However, when present, metastatic disease is found in up to 30% of somatostatinomas in patients with NF-1 (22).

**Published online**
10.1148/radiol.12112512 **Content codes:** GI CT MR NM

**Radiology 2013;** 266:38–61

**Abbreviations:**
ADC = apparent diffusion coefficient
GEP-NET = gastroenteropancreatic NET
MEN-1 = multiple endocrine neoplasia type 1
NET = neuroendocrine tumor
NF-1 = neurofibromatosis type 1
SRS = somatostatin receptor scintigraphy
SSTR = somatostatin transmembrane receptor

Conflicts of interest are listed at the end of this article.

**Table 1**

**Incidence and Main Clinical Characteristics of Most Common GEP-NETs in Relation to Their Site**

| Site* | Percentage of NETs | Percentage of All Neoplasms | Malignancy (%) | Main Clinical Characteristics† |
|---|---|---|---|---|
| Pancreas | 7 | 1–10 | | Incidence peaks at age 60–70 years; 5-year survival < 40% |
| Nonfunctioning | Up to 60–80 | … | 60%–80% | Characteristically large (mean, 4 cm); diagnosed mostly on basis of mass effect (pancreatitis, abdominal pain, jaundice, weight loss) |
| Functioning | | | | |
| Insuloma | *32* | … | 10% | 90% are <1–2 cm; 10% are multiple (generally in MEN-1); rarely have extrapancreatic location |
| Gastrinoma | *9* | … | 60%–90% (pancreatic tumors reported as more aggressive than duodenal) | Frequently < 1 cm and in the duodenum (less common in pancreas); multiple in MEN-1 and ZES |
| Glucagnomas | Rare | … | Frequently | Generally single; almost entirely intrapancreatic in location; large (mean, 6 cm); with liver metastases in 60% of cases at diagnosis |
| VIPoma | Rare | … | Frequently | Usually single; 95% intrapancreatic; metastatic at presentation in 70%–80% of cases |
| Somatostatinomas, others | Rare | … | Malignancy rate higher in pancreatic duodenal tumors | Usually single; 50% pancreatic, remainder in duodenum and/or small intestine; 50%–60% malignant |
| Extrapancreatic | | | | |
| Stomach | 6–9 | 1 | … | … |
| Type I | 70-80 of stomach NETs | … | Rarely invasive | Incidence peak mean age, 63 years (>women); associated with chronic atrophic gastritis/ pernicious anemia; often multifocal; lesions < 2 cm treated with endoscopic resection; >2 cm, recurrent, or >6 lesions treated with local surgical resection |
| Type II | 5–6 of stomach NETs | … | Rarely invasive | Incidence peak mean age 50 years; associated with ZES; often multifocal; lesions < 2 cm treated with endoscopic resection; >2 cm, recurrent, or >6 lesions treated with local surgical resection |
| Type III | 15–20 of stomach NETs | … | Most malignant; often manifests with metastases (50%–70% of well differentiated, up to 100% of poorly differentiated) | Incidence peak mean age 55 years (>men); solitary lesion; treated with partial gastrectomy, nodal dissection |
| Small intestine | | 33 | | Peak incidence mean age 80 years |
| Duodenum and upper jejunum | 2–3 (22% of all small-bowel NETs) | … | Early regional nodal metastases (11%–50%, up to 90% in functioning gastrinomas). | Majority are well differentiated; poorly differentiated rare (1.8%, > ampullary carcinomas); 62% gastrin cell tumors (one-third functional); multiple when associated with MEN-1/ZES; common symptoms: ZES, abdominal pain (37%), bleeding (21%), anemia (21%), jaundice (18%, up to 60% in periampullary region; locally resected if small, Whipple procedure if larger; 10-year survival rate 59% for duodenal gastrinomas vs 9% for pancreatic tumors |

Table 1 (continues)

**Table 1 (continued)**

**Incidence and Main Clinical Characteristics of Most Common GEP-NETs in Relation to Their Site**

| Site* | Percentage of NETs | Percentage of All Neoplasms | Malignancy (%) | Main Clinical Characteristics† |
|---|---|---|---|---|
| Ileum | 30 (>70% of all small-bowel NETs, generally in distal ileum) | … | Up to 20% with hepatic metastases (even when primary tumor is small). | Sporadic incidence age; multiple lesions in 26%–40% and associated with other noncarcinoid malignancies in 15%–29%; most patients symptomatic: intermittent/partial obstruction, abdominal pain; classic carcinoid syndrome in 6%–30% (associated with hepatic metastases in >95% of cases); 5-year survival: 36% (distant metastases) to 65% (localized regional disease) |
| Colon | Rare | … | Generally aggressive (most poorly differentiated). | More common in right side of colon, with large lesions (mean, 5 cm) |
| Rectum | 21–27 | 1 | 82% localized at time of diagnosis; metastases in 2% of lesions <2 cm. | Peak incidence mean age 50 years; typically small (<1 cm) and asymptomatic; most in midrectum, 5–10 cm from anal verge; high 5-year survival rate (88%) |
| Appendix | 17–20 | 60 | Generally benign (up to 70% incidentally found at appendectomy). | Mostly increased incidence around age 40 years and in female. High 5-year survival rate (>80%) |

Note.—GEP-NETs are generally rare relative to prevalence of other epithelial neoplastic counterparts, with the exception of those arising in the ileum and appendix. Malignancy of GEP-NETs is related not only to grade and stage but also to origin: tumors arising from small bowel or type III gastric NETs are generally more frequently malignant than pancreatic insulinomas, appendiceal NETs or type I/II gastric carcinoids (1,3–8,13–16,21,63,86,88,100,101).

* In the foregut, 41% of cases are in United States; 30.4%, in Japan; esophagus, stomach, first two-thirds of duodenum, liver, gallbladder, pancreas, spleen. In the midgut, 26% of cases are in United States; 9.6%, in Japan: last one-third of duodenum, jejunum, ileum, appendix, cecum, ascending colon, hepatic flexure of colon, transverse colon. In the hindgut 19% of cases are in United States; 60%, in Japan: distal one-third of transverse colon, splenic flexure, descending colon, sigmoid colon and rectum (7,12).

† MEN-1 = multiple endocrine neoplasia type 1, ZES = Zollinger-Ellison syndrome.

## Diagnosis

The diagnosis of a GEP-NET and its subsequent investigation is dependent on clinical presentation and tumor location. In patients with symptoms due to hormone hypersecretion, laboratory analyses are crucial and specific neuroendocrine hormone levels (ie, gastrin, insulin, products of serotonin metabolism) should be tested in the serum and in the urine (8,16,18,26). Chromogranin A is the most commonly used neuroendocrine serum marker, with a reported sensitivity and specificity of 68% and 86%, respectively. Elevated chromogranin A levels have been found in 60%–80% of GEP-NETs (10) and are associated with higher tumor burden (18,27); levels also depend on location (higher levels in ileal NETs and in those associated with MEN-1) and degree of differentiation (higher in well-differentiated NETs). A falsely elevated chromogranin A level is commonly seen in patients treated with proton-pump inhibitors, although the reason for this direct relationship is not yet clearly understood (28).

Histopathologic analysis is required to confirm the diagnosis (26), which relies on the demonstration of neuroendocrine markers in the tissue (4,10,17,29). The current guidelines recommend immunolabeling for general neuroendocrine markers such as synapthophysin and chromogranin A for the diagnosis (4,17): Chromogranin A is the most widely used marker of neuroendocrine differentiation (5), and synapthophysin is a sensitive but nonspecific marker expressed by adenomas and carcinomas of the adrenal cortex and normal cells (30). However, their expression is limited in poorly differentiated NETs (21).

## Pathologic Classification and Staging

Owing to their complex biologic characteristics, a simple classification of NETs as benign or malignant is insufficient to estimate their prognosis or to select an appropriate treatment and monitoring approach. Knowledge of tumor grade and differentiation is essential to understand tumor biology and stratify the patient's risk for metastases and recurrence. Poorly differentiated or high-grade tumors can manifest with concurrent metastasis in 50% of cases (2,7,29).

The initial classification proposed by World Health Organization in 2000 relied on tumor cell differentiation alone (29) to stratify NETs into three broad categories (2,31). In 2005, the European Neuroendocrine Tumor Society (ENETS) introduced new guidelines that factored TNM staging (tumor location and size, local invasion, nodal and distant metastases), as well as tumor grade (proliferative index) (4,8,16,32,33), mitotic count, and Ki-67 labeling index (32–34). With the increasing use of the ENETS guidelines and the recognized limitations of

**Table 2**

**Association of GEP-NETs with Complex Autosomal Dominant Genetic Syndromes**

| Syndrome | Location of Gene Mutation | Main Clinical Features | Notes |
|---|---|---|---|
| MEN-1 | 11q13; menin gene is TSG | Primary hyperparathyroidism (> 95%): parathyroid hyperplasia or adenomas (initial manifestation, usually in 3rd decade of life); pancreatic NETs (25%–75%): nonfunctioning (20%–30%), gastrinomas (25%), insulinomas (< 5%); pituitary tumors (20%–40%); others: thymus and lung NETs, gastric carcinoids (0%–10%) | Mean age at diagnosis, ~30 years (~15 years in screened families);diagnosis requires presence of at least two of three classic lesions (parathyroid, pancreas, pituitary); nonfunctioning pancreatic NETs usually in early ages; gastrinomas/other functioning after age 40 years; malignant pancreatic NETs most common cause of death (reported malignancy rate, 40%–60% for gastrinomas, 27% for nonfunctioning) |
| Von Hippel–Lindau syndrome | 3p25–26 | Retinal or central nervous system hemangioblastoma (21%–72%); renal cell carcinoma (predominantly clear cell) incidence as high as 75%; pancreatic involvement (20%–75%): cystic tumors (70%–91%), NET (10%–17%; most often multiple; 98% nonfunctioning); pheochromocytoma (7%–18%; up to 90% in some series) | Mean age at diagnosis of pancreatic NET, 29–38 years; renal cell carcinoma (frequently bilateral, multicentric, solid): 50% of deaths; not infrequent metastasis from renal cell carcinoma to pancreas; hemangioblastomas: major cause of morbidity and mortality (rupture, bleed, mass effect); pheochromocytomas: tumors frequently bilateral, rarely malignant |
| NF-1 | 17q11.2 | Neurofibromas, optic gliomas (15% in children <6 years old), dysplastic bone lesions; duodenal/periampullary and pancreatic somatostatinomas (1%, generally nonfunctioning); pancreatic gastrinomas, insulinomas and nonfunctioning reported; pheochromocytoma and paraganglyomas (1%–5%) | Two- to four-fold higher risk of developing tumors than general population (risk of malignancy, 5%–15%); somatostatinomas: associated with biliary dilatation, pancreatitis, jaundice, nausea, pain, bleeding, vomiting; metastasis (nodes or liver) in about 30% of somatostatinomas |
| Tuberous sclerosis complex | 9q34 (TSC-1 is TSG) and 16p13.3 (TSC-2 is TSG) | Facial angiofibromas, retinal hamartomas, astrocytomas, angiomyolipomas (major features); pituitary tumors, parathyroid involvement (adenoma and hyperplasia) (rare); pancreatic NETs (rare): nonfunctioning, gastrinomas and insulinomas. | In children, 18-fold higher risk of malignancy than in general population; neuroendocrine tumors not considered one of major features |

Note.—Point mutations, deletions, methylation, and chromosomal losses and gains in the TSGs have been shown to be involved in the development of these tumors. For example, deletions and mutations of 11q13 (*MEN1* or menin gene), are noted in 70%–90% of MEN-1 families. Losses of chromosome 1,11q and gains on 9q are early events in the development of pancreatic NET. NETs, particularly in pancreas are more common in patients with MEN-1 or Von Hippel–Lindau syndrome than in those with NF-1 (1%) and tuberous sclerosis complex (rare) (4,9,10,16,21–23,25,86). TSG = tumor suppressor gene.

the initial classification system, the World Health Organization classification was modified in 2010 to include tumor grade and differentiation in the criteria (Table 3) (4,21,35). In the same year, a consensus was developed to encourage pathologists to include the essential pathologic features (ie, grade and stage) for each pathologist's interpretation (4,36).

## Imaging Techniques

To appropriately care for patients affected by GEP-NETs, accurate detection and characterization of the primary lesion, as well as determination of local extent and presence of metastases, are required along with evaluation of somatostatin transmembrane receptor (SSTR) density. Likewise, treatment monitoring and recurrence detection are also important clinical objectives. The choice and subsequent role of imaging techniques is dependent on tumor status at the time of presentation (11).

### Noninvasive Techniques: Morphologic Imaging

Transabdominal ultrasonography (US) is a readily available noninvasive technique that could be used in thin patients to screen the solid organs in the abdomen. However, its role is generally limited in the evaluation of the pancreas due to the presence of overlying bowel gas and other structures that often impede optimal evaluation, particularly of the pancreatic body and tail (3,11). NETs typically appear on US images as a hypoechoic mass surrounded by a hyperechoic halo (3). Overall, US has limited sensitivity for the detection of GEP-NETs, with reported values of 13%–27% (37).

Multidetector computed tomography (CT) is a widely available technique with

high spatial and temporal resolution; therefore, it represents the most common initial imaging test to evaluate for suspected pathologic conditions in the abdomen (Table 4) (4). Its rapid acquisition speed and capabilities for thin collimation, multiplanar reconstructions, and image display in the desired plane enable improved lesion detection and provide anatomic details for surgical planning (3,38). The multidetector CT acquisition parameters and the iodinated contrast media injection protocols can be tailored to survey multiple body parts or serve as a focused examination to meet a specific clinical need or for preoperative workup. Moreover, surgeons and oncologists are more familiar in interpreting CT images for decision making.

For small-bowel tumors, CT enterography can be performed after the small bowel is distended with a large volume of neutral or low-attenuating oral contrast medium (39). Unenhanced scans are generally performed to evaluate for the presence of calcification or hemorrhage within the lesions and to plan the cranial-to-caudal extent for the subsequent dynamic phase acquisitions following contrast agent injection. As GEP-NETs and their metastases are often hypervascular, they are usually more conspicuous in the early arterial phase of the acquisition (40,41). A multiphase acquisition is, therefore, more appropriate to evaluate these tumors (42,43). However, the performance of CT is influenced by the scanning protocols, as well as the lesion size, location, and contrast with the surrounding tissue. Therefore, the sensitivity of CT for small lesion detection and characterization in the abdomen can be lower (1,3,44). Owing to its increased use in clinical practice, ionizing radiation exposure is another concern with CT, especially in younger patients. However, several technical approaches are now being used to lower radiation dose such as automated tube current modulation, the use of lower tube voltage for the arterial phase acquisition, reduction in the number of acquisition phases, or elimination of the unenhanced phase, as well as newer image reconstruction methods. Moreover, focusing coverage on a specific region of interest may also be helpful in dose reduction.

In comparison, magnetic resonance (MR) imaging offers superior intrinsic soft-tissue contrast combined with multiplanar acquisitions for improved lesion detection and characterization (3,21,38,45,46). Recent advances in the MR imaging hardware and software have also improved the spatial resolution and acquisition time for each sequence, resulting in shorter breath holds (38). Furthermore, MR imaging does not use ionizing radiation (3). However, MR imaging is less readily available, is more expensive, and often requires more time and patient cooperation. Currently, MR imaging is best performed as a focused examination for each body part (eg, detection of liver metastases) to obtain images with higher spatial resolution by using appropriate timing acquisition after contrast agent injection and avoiding patient motion. Hence, screening multiple regions for metastatic disease in the same examination is not routinely undertaken, and MR imaging is best used as a problem-solving tool in patients with negative or equivocal findings from other imaging techniques, such as CT (11). MR imaging can also be used to screen young patients at risk for developing NETs (22,23). Most NETs are of low signal intensity on T1-weighted MR images and hyperintense on T2-weighted images (3,21,39,46,47). However their characteristics on MR images depend on cellular composition and tumor biology. On contrast-enhanced MR images, these tumors are often hypervascular in the arterial phase and show varying degrees of heterogeneity, depending on tumor size and behavior. For example, fast-growing NETs with an aggressive behavior tend to show cystic changes and necrosis in their contest. Such necrotic and cystic components generally demonstrate higher signal intensity and appear as low-signal-intensity areas on contrast-enhanced images (3,39,43,44).

## Noninvasive Techniques: Functional Imaging

*Somatostatin receptor imaging.*—Since NETs often manifest with increased expression of SSTR at the cell membrane (70%–90% of carcinoids and 50%–80% of pancreatic NETs, mostly in well-differentiated tumors) (47–51), receptor-targeted functional imaging can be performed. Currently, five main subtypes of SSTR have been identified in humans (SSTR-1, SSTR-2A and SSTR-2B, SSTR-3, SSTR-4, and SSTR-5). SSTR-2 is the predominantly expressed one (49,52,53). Somatostatin receptor scintigraphy (SRS) is based on the high affinity of synthetic somatostatin analogs for tissue expressing SSTR. Octreotide, the first commercially available somatostatin analog, was introduced 2 decades ago and was labeled with indium 111 ($^{111}$In pentetreotide, OctreoScan; Mallinckrodt Medical, St Louis, Mo) to help diagnose receptor-positive lesions by using scintigraphy (3,52) It is still considered the reference standard for functional imaging of NETs (3). By combining single-photon emission computed tomography (SPECT) with planar imaging, the spatial resolution of octreotide imaging has been improved (16). Nonspecific uptake in inflammatory tissue or in normal structures (adrenals, thyroid, spleen, pituitary, liver, kidneys) and poor intrinsic spatial resolution are two recognized limitations of somatostatin receptor scintigraphy (54,55). In addition, the time required between radiotracer injection and image acquisition is about 24–48 hours (10,55).

*Positron emission tomography (PET).*—Novel somatostatin analogs have been subsequently developed to overcome the limitations of octreotide imaging. These analogs allow radiolabeling with positron-emitting tracers that can be used with PET/CT (10,55). These include gallium 68–tetraazacyclododecane tetraacetic acid–octreotate ($^{68}$Ga-DOTA-TATE [SSTR-2 analog]), $^{68}$Ga-edotreotride (SSTR-2 and SSTR-5 analog) and $^{68}$Ga-DOTA-NOC, also known as [$^{68}$Ga]DOTA-[Nal$^3$]-octreotide (SSTR-2, SSTR-3, and SSTR-5 analog). Octreotide analogs labeled with $^{68}$Ga directly bind SSTR and are rapidly excreted from nontarget sites. Their uptake is related both to the extent of somatostatin-receptor expression on tumor cell membranes and to their affinity to SSTR. In particular, these

**Table 3**

**European Neuroendocrine Tumor Society and World Health Organization 2010 Classification Systems for NETs**

| Differentiation | Grade | Grading System | ENETS Nomenclature | WHO 2010 Nomenclature |
|---|---|---|---|---|
| Well differentiated | Low (ENETS G1) | <2 mitoses/10 HPFs and Ki-67 index < 3% | NET, grade 1 (G1) | Neuroendocrine neoplasm, grade 1 |
| Well differentiated | Intermediate (ENETS G2) | 2–20 mitoses/10 HPFs or Ki-67 index = 3%–20% | NET, grade 2 (G2) | Neuroendocrine neoplasm, grade 2 |
| Poorly differentiated | High (ENETS G3) | >20 mitoses/10 HPFs Ki-67 index > 20% | Neuroendocrine carcinoma, grade 3 (G3), small cell carcinoma; neuroendocrine carcinoma, grade 3 (G3), large cell carcinoma | Neuroendocrine carcinoma, grade 3, small cell carcinoma; neuroendocrine carcinoma, grade 3, large cell neuroendocrine carcinoma |

Source.—Reference 29.

Note.—Differentiation refers to extent to which neoplastic cells resemble their nonneoplastic counterparts (eg, well-differentiated NETs have characteristic "organoid" morphology: Cells are uniform and produce abundant neurosecretory granules [21]). Tumor grade (or proliferative index) refers to biologic aggressiveness of the tumor. For pancreatic tumors, low grade is defined as fewer than mitoses/50 HPFs and nonnecrosis; intermediate grade, as two to 50 mitoses/50 HPFs or foci of necrosis; and high grade, as more than 50 mitoses/50 HPFs (4).Well-differentiated low-grade (G1) neoplasms (*NETs* in 2000 WHO classification) demonstrate benign or uncertain malignant behavior; well-differentiated intermediate-grade (G2) neoplasms (*neuroendocrine carcinomas* in 2000 WHO classification) demonstrate low grade of malignancy. Poorly differentiated (G3) lesions include small cell and large cell carcinoma variants; generally, these lesions demonstrate aggressive behavior. Today, the term *carcinoid* is usually referred to the serotonin-producing GEP-NETs of the ileum or appendix leading to carcinoid syndrome, while the other tumor types are termed *NETs* followed by their primary location (2,4,21,29,32,33,35). ENETS = European Neuroendocrine Tumor Society, HPF = high-power field, WHO = World Health Organization.

**Table 4**

**Multidetector CT Imaging Protocols for GEP-NETs**

| | | Contrast Agent Enhanced† | | |
|---|---|---|---|---|
| Site | Unenhanced * | Arterial Phase‡ | Venous Phase* | Preparation |
| Pancreas | Upper abdomen | Upper abdomen; 45 sec after contrast agent injection. | Upper abdomen and pelvis | None |
| Extrapancreatic | | | | |
| Duodenum | Upper abdomen | Upper abdomen; 35 sec after contrast agent injection. | Upper abdomen and pelvis | Bowel distention with 500 mL of water before scan |
| Ileum | Upper abdomen and pelvis | Upper abdomen and pelvis; 35 sec after contrast agent injection. | Upper abdomen | Bowel distention (CT enteroclysis) with 1500–2000 mL of water with 0.5% osmotic solution 1 hour before scan |
| Colon | Upper abdomen and pelvis | Upper abdomen and pelvis; 35 sec after contrast agent injection. | Upper abdomen | None |
| Rectum | Upper abdomen and pelvis | Upper abdomen and pelvis; 35 sec after contrast agent injection. | Upper abdomen | None |
| Appendix | Upper abdomen and pelvis | Upper abdomen and pelvis; 35 sec after contrast injection | Upper abdomen | None |

Note.—Upper abdomen scan performed through liver and pancreas. Unenhanced scan is acquired before contrast agent injection to evaluate for presence of calcification and hemorrhage in the lesion and to plan range of scan for dynamic phase CT. Arterial phase should be planned to enable detection of hypervascular primary tumor and liver metastases. Focusing scan coverage on specific region of interest might help reduce radiation dose (of particular importance in young patients).

* Section thickness = 5 mm.

† Intravenous contrast agent volume is 100–120 mL injected at rate of 4–5 mL/sec.

‡ Section thickness = 1.25–2.5 mm.

analogs have high affinity to SSTR-2 but lower affinity to other subtypes (eg, SSTR-3 and SSTR-5). The scanning can be performed within 45–90 minutes after radiotracer injection (10,48,56). Moreover, hybrid PET/CT scanners, now more widely available in clinical practice, allow better spatial resolution, and both PET and contrast-enhanced multidetector CT studies can be obtained in the same setting (54,56). However, higher costs and the fact that the availability of $^{68}$Ga generators is limited to specialized centers remain impediments to their routine use in clinical care (10).

**Figure 1**

**Figure 1:** Coronal reconstruction contrast-enhanced arterial phase CT image of functioning pancreatic NET in a young woman shows pancreatic insulinoma (arrow) with typical imaging features such as small size (9 mm) and avid enhancement.

**Figure 2**


a. b.

**Figure 2:** Coronal reconstruction contrast-enhanced CT images in a 54-year-old man with Zollinger-Ellison syndrome and increased serum levels of gastrin. **(a)** A 4.8-cm enhancing mass is visible posterior to the uncinate process (straight arrow), as are pathologically enlarged and avidly enhancing regional lymph nodes (arrowheads). Curved arrow = nasogastric tube in stomach. **(b)** Thickening of folds in stomach (arrows) and jejunal wall (arrowheads) are also evident. Mass was diagnosed as low-grade well-differentiated pancreatic NET. Primary tumor stained positive for chromogranin, synaptophysin, and gastrin (not shown).

Tumor metabolic imaging has been already popularized with the acceptance of fluorine 18 fluorodeoxyglucose (FDG) PET/CT as the oncologic imaging test of choice for many neoplasms. FDG is a glucose analog is taken up by cells that use glucose for their metabolic activity, but subsequent phosphorylation prevents its release from the cells. FDG PET has limited value in well-differentiated NETs, because these tumors often have an almost normal glucose turnover. However, FDG PET appears to be a promising marker of tumor aggressiveness and metastatic disease in NETs (3,4,48,49,57–59).

### Invasive Techniques

Endoscopic US allows the use of higher frequency (7.5–12-MHz) probes positioned in proximity to the organ of interest (3)—generally stomach, pancreas, duodenum, and rectum—thereby providing an opportunity to depict small lesions not visible on images obtained with other imaging methods. The reported detection rate of endoscopic US is 45%–60% for duodenal lesions and 80%–100% for pancreatic NETs (21,60–62). Also, endoscopic US performance is superior in the proximal portion of the pancreas (83%–100%) than in the distal body and tail (37%–69%) (24,61). The terminal ileum can also be interrogated with endoscopic US by using high-frequency miniature probes passed through the biopsy channel of the colonoscope (63). Endoscopic US allows for concurrent fine-needle aspiration (FNA) of the lesions and adjacent lymph nodes, but this technique is invasive. Other drawbacks of endoscopic US are operator dependency and the limited field of view, which can affect its performance in the detection of lesions outside the area of immediate interest. In addition, pathologists are not always comfortable in classifying NETs as benign or malignant on endoscopic US–guided FNA samples, with an overall accuracy of 40%–47%; in particular, lesions with uncertain behavior are challenging (64,65).

Gastroduodenoscopy and colonoscopy play a fundamental role in gastrointestinal tract NETs, even for their treatment when small and localized (11). Double-balloon enteroscopy and video capsule endoscopy are two relatively new techniques for endoscopic examination of jejunum and ileum; these methods have been shown to be capable of localizing small intestinal NETs not detected with the aid other modalities (66), even in patients with metastatic disease (1,10).

## Role of Imaging in Tumor Detection and Characterization

### Pancreatic NETs

Nonfunctional tumors currently account for the majority of newly diagnosed pancreatic NETs (up to 60%–80%) (3,68), whereas insulinomas (32%) are the most common functioning islet cell tumors, followed by gastrinomas (9%) (16,21,68).

A multiphase multidetector CT examination is an accepted first-line imaging test to evaluate the pancreas for suspected lesions (4,16,21). Moreover, the technologic advances in multidetector CT have also improved the detection rate of NETs from a range of 14%–30% (reported in older studies) to 69%–94% in recent studies (11,43,69–73). Functioning NETs are generally small (1–2 cm) and manifest as well-defined, hypervascular lesions owing to their rich capillary network (Figs 1, 2). The larger tumors (eg, glucagonomas) often demonstrate degeneration and heterogeneity (6,21,74,75). Nonfunctioning tumors, on the other hand, are relatively larger in size (mean, 4 cm) at the time of detection (6,16), are often well defined and encapsulated and show heterogeneous enhancement. This finding is due to areas of cystic degeneration, necrosis, and, less frequently,

**Figure 3**

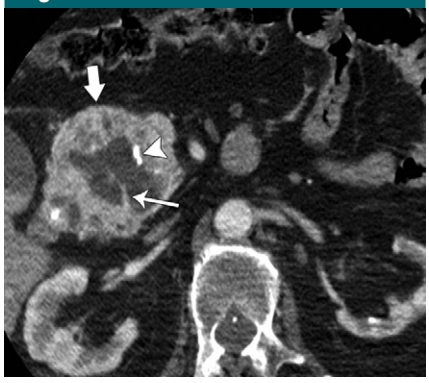

**Figure 3:** Axial contrast-enhanced CT image in a 75-year-old man shows well-defined, arterially enhancing, solid and cystic mass (thick arrow) in the pancreatic head, with calcifications (arrowhead), irregular thick enhancing wall, and inner septum (thin arrow). This lesion was found incidentally. Surgical diagnosis was well-differentiated NET with foci of poorly differentiated neuroendocrine carcinoma (G3: more than 20 mitoses per 10 high-power fields, Ki-67 index > 20%).

**Figure 4**

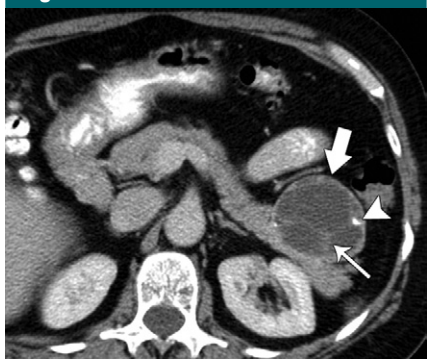

**Figure 4:** Axial contrast-enhanced arterial phase multidetector CT image in a 62-year-old woman with abdominal pain and weight loss shows large (5.5-cm) predominantly cystic mass (thick arrow) with thin septa (thin arrow) and calcifications (arrowhead) in pancreatic tail. This mass was confirmed as a well-differentiated nonfunctioning pancreatic NET at surgical pathologic evaluation.

**Figure 5**

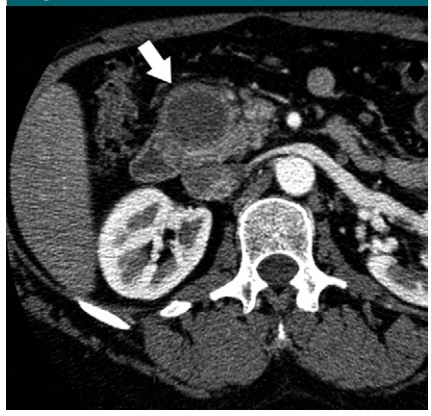

**Figure 5:** Axial contrast-enhanced multidetector CT image in 47-year-old woman who presented with abdominal pain shows NET with complete cystic degeneration (arrow) in pancreatic head. At pathologic examination, there were no malignant changes in this tumor.

fibrosis (Figs 3, 4) (6,38,74). Occasionally, they are completely cystic (Fig 5) but typically demonstrate a hypervascular rim in up to 90% of cases (74). In one series, cystic NETs composed 17% of all pancreatic NETs and were larger than solid tumors; moreover, they were more likely to be symptomatic and 3.5 times more common than solid tumors in patients with MEN-1 (76). Aggressive tumors often demonstrate local invasion into the retroperitoneum, and metastases (up to 80% of cases) to the regional lymph nodes and the liver are commonly observed (6). A statistically significant correlation has been reported (74,75) between large tumor size and the presence of distant metastases, local and vascular invasion (generally arterial, rarely venous encasement), and calcification. Moreover, calcification, when present (up to 20% of nonfunctioning NETs), is often indicative of a malignant lesion. Usually, pancreatic NETs do not cause pancreatic or biliary duct obstruction, but they can involve the main pancreatic duct on rare occasions, which results in severe dilatation of the upstream tract of that duct (75,77). When incidentally detected, NETs are often small (median, 3 cm), and those measuring larger than 2 cm are often benign (78–80).

The above described morphology on CT images can also be seen on MR studies. In addition, pancreatic NETs appear as relatively hypointense masses on T1-weighted MR images (both with and without fat saturation) and generally demonstrate high signal intensity on T2-weighted images (74). Moreover, the superior soft-tissue contrast of MR imaging can improve detection and characterization of challenging NETs (Fig 6). MR imaging has an overall sensitivity of 74%–94% and specificity of 78%–100% (43,69,81). MR techniques such as diffusion-weighted imaging and apparent diffusion coefficient (ADC) mapping now serve a complementary role to other MR sequences, particularly for localizing nonhypervascular tumors (Fig 7) (82). In one study an inverse correlation between tumor Ki-67 labeling index on pathology and ADC values was demonstrated, supporting the role of diffusion-weighted imaging in helping predict tumor biology (83). If validated, this property of diffusion-weighted imaging could be used in monitoring small incidental NETs and tumors detected on screening studies in high-risk patients.

Hypervascular metastases to the pancreas from renal cell carcinoma, solid serous cystadenomas, and intrapancreatic accessory spleen (IPAS) in the pancreatic tail share some imaging features with NET (25,38,84,85). MR imaging can enable IPAS characterization, because IPAS usually manifests signal intensity characteristics on images obtained with all MR sequences and enhancement features similar to those of the spleen (84). Otherwise, heat-damaged technetium 99m–red blood cell scintigraphy with single photon emission computed tomography (SPECT)/CT can be useful in diagnosis of IPAS owing to specific radiotracer uptake in splenic tissue.

Endocscopic US is generally performed in patients with equivocal or negative CT/MR findings when NET is clinically suspected (Fig 8). In experienced hands, endoscopic US combined with biopsy is the most sensitive method to help detect pancreatic NETs (sensitivity and accuracy > 80%), particularly lesions smaller than 2 cm (62,67,86). A recent study has shown that the sensitivity of endoscopic US is greater than that of CT (91.7% vs 63.3%), particularly for insulinomas (84.2% vs 31.6%) (67). Tumors with negative CT findings are usually small

**Figure 6**

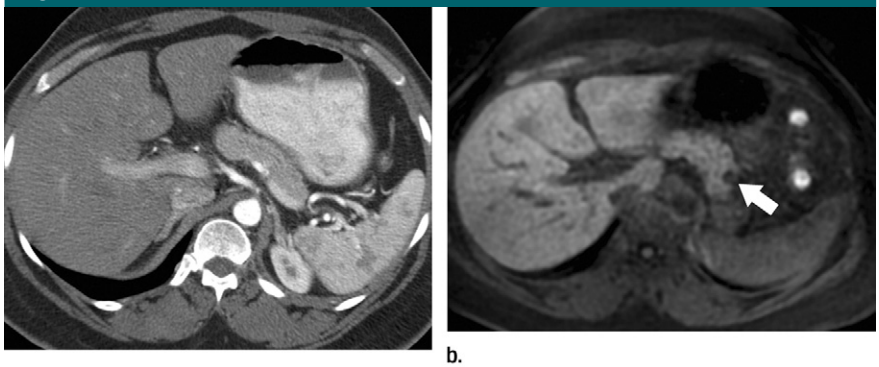

a.

b.

c.

**Figure 6:** Axial images in a 51-year-old woman with vague abdominal pain and weight loss. **(a)** Contrast-enhanced arterial phase CT image thorough pancreatic body and tail does not reveal any abnormality in the pancreas. **(b)** Unenhanced T1-weighted fat-saturated (repetition time msec/echo time msec/inversion time msec, 2.348/1.048/7; flip angle, 12°) and **(c)** contrast-enhanced (2.348/1.048/7; flip angle, 12°) MR images show small (6-mm) hypointense lesion in superior aspect of the pancreatic body in **b** (arrow) with intense contrast enhancement in **c** (arrow). Patient underwent laparoscopic enucleation of lesion. At pathologic examination, diagnosis of nonfunctioning well-differentiated low-grade NET was confirmed.

**Figure 7**

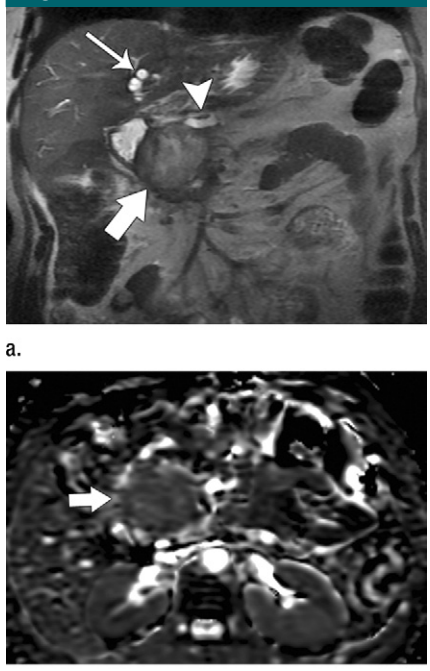

a.

b.

**Figure 7:** Malignant nonfunctioning NET in a 58-year-old man. **(a)** Coronal T2-weighted MR image (repetition time msec/echo time msec, 1538/77.62; flip angle, 90°) and **(b)** axial ADC map (*b* values, 0 and 600 sec/mm$^2$; 3000/66.4, flip angle, 90°) show large (8.4-cm) mass in pancreatic head with mild hyperintensity (large arrow), dilatation of main pancreatic duct (arrowhead) and intrahepatic bile ducts (thin arrow) on **a.** Tumor showed restricted diffusion (low signal intensity; arrow) on **b.** CT-guided biopsy revealed neuroendocrine carcinoma.

**Figure 8**

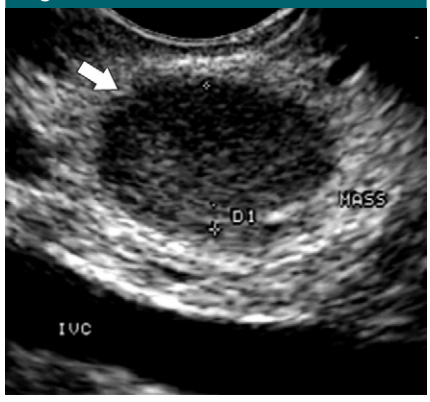


**Figure 8:** Endoscopic US image in a 43-year-old man suspected of having a pancreatic lesion but with unremarkable contrast-enhanced CT findings (not shown). Endoscopic US performed for lesion detection showed small, hypoechoic, well-defined lesion in duodenal wall (arrow). Endoscopic US–guided biopsy helped diagnose gastrinoma.

and are more likely to be insulinomas. Hence, a sequential approach of CT followed by endoscopic US can help detect virtually all pancreatic NETs (61,67).

Although pancreatic NETs overexpress somatostatin receptors (21,69) the role of SRS functional imaging is limited, because, once detected, the majority would directly be surgically resected. However, where the primary tumor is elusive or in patients with metastatic disease, functional imaging has a role in tumor detection and targeted therapy selection. The sensitivity for detection of pancreatic NETs (nonfunctioning, gastrinomas, glucagonomas) ranges from 75% to 100% (16,38,49,73) but is lower (14%–53%) for insulinomas because they insufficiently express SSTRs (50%–60%) (Fig 9) (16,38,73).

### Extrapancreatic NETs

NETs that arise in the gastrointestinal tract represent the majority (67%) of NETs (6), and the distal part of the ileum is the most frequent (up to 30%) site of GEP-NETs (5,7). The preoperative detection of a primary tumor in the gastrointestinal tract is challenging because of the typically small tumor size (87), the length of the tract, and its tortuous course. The localization of ileal carcinoids can be particularly challenging; furthermore, they are multifocal in 26%–40% of cases (4,6,10,38,63).

Gastric NETs are mostly composed of enterochromaffin-like cells (86,88). Three types have been described (14,86): Type 1 (70%–80%) and type II (6%) are associated with hypergastrinemia and usually manifest as multiple small (<1–2 cm) benign polyps in the gastric fundus and body (6,88). They are usually asymptomatic

**Figure 9**

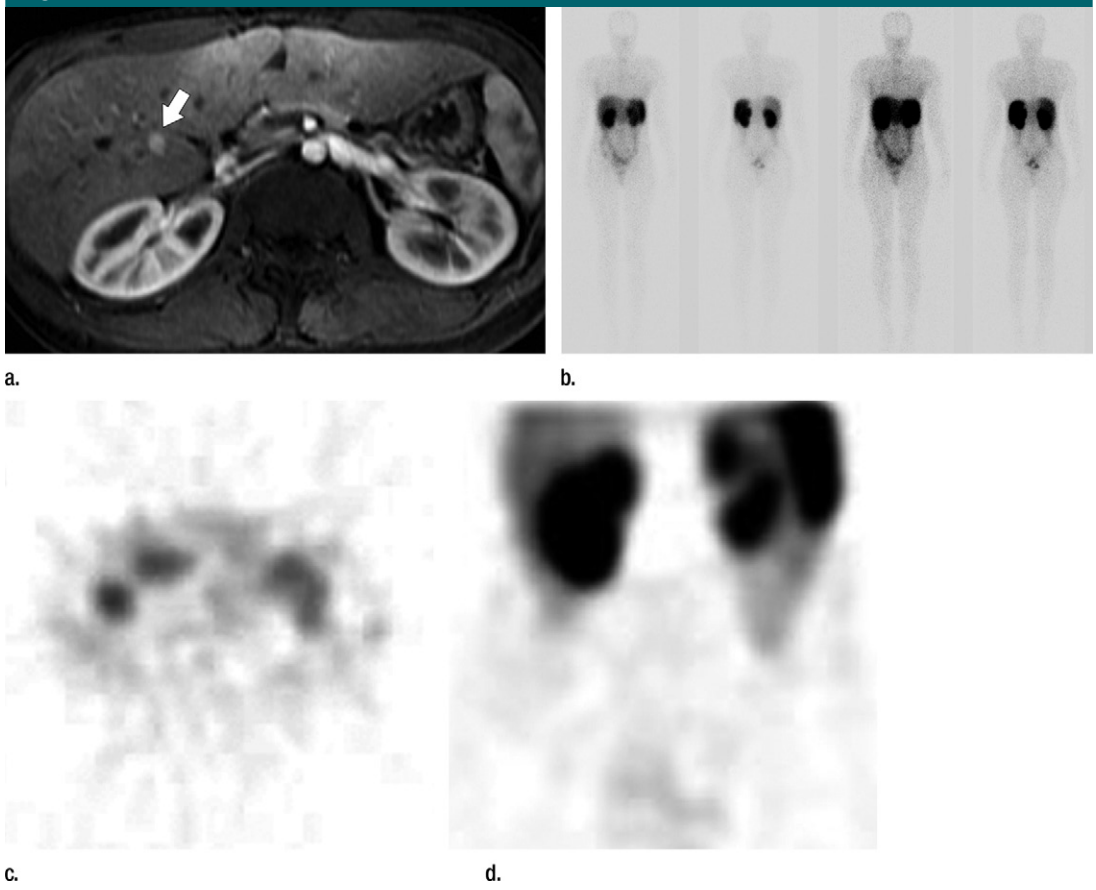


**Figure 9:** Metastatic insulinoma with negative octreotide scan findings in a 15-year-old girl who underwent distal pancreatectomy (primary not shown). **(a)** Axial contrast-enhanced MR image (175/1.8; flip angle, 90°) performed 2 years after surgery for a new hypoglycemic event shows a small arterially enhancing lesion (arrow) in right lobe of liver. **(b)** Octreotide whole-body scan and **(c)** axial and **(d)** coronal SPECT images obtained 24 hours after injection of 222 MBq $^{111}$In-octreotide: No focal areas of uptake in liver are seen. Patient underwent partial hepatectomy but developed additional lesions a few months later. Finally, orthotropic liver transplantation was performed. Octreotide scanning has reduced sensitivity for insulinomas due to limited expression of somatostatin receptors at tumor cell membrane.

and are often incidentally discovered at endoscopy (6). Type III gastric NETs (13%–20%) are sporadic and not associated with hypergastrinemia. They manifest as a large (>2-cm) solitary mass in the gastric body and fundus and have an increased risk of spread to regional lymph nodes and liver metastases (reported as 50%–70% in well-differentiated and up to 100% in poorly differentiated cases). Patients often present with symptoms related to an aggressive mass or with upper gastrointestinal tract bleeding (5,6,88–90). Gastroscopy and endoscopic US are essential to localize the primary lesion for histopathologic diagnosis (86). Furthermore, tumor invasiveness through the gastric wall can be reliably studied with an endocscopic US examination (21). On contrast-enhanced CT images, type I and type II tumors appear as numerous enhancing submucosal lesions similar to other small gastric tumors and polyps (6,88). Stomach distention with a neutral-attenuation oral contrast agent such as water is advised to improve the detection of small lesions at contrast-enhanced CT (21). Type III lesions demonstrate an infiltrative morphology similar to that seen in adenocarcinomas and often show avid enhancement (5,6,88). In patients with type I or type II tumors that are smaller than 2 cm or those with type III disease and poorly differentiated lesions, contrast-enhanced CT and/or MR imaging are mostly important for staging distant metastases (21,24,86).

Duodenal NETs are rare (2%–3%) (4–6) and often incidentally diagnosed at gastroduodenoscopy, predominantly in the upper portion of the duodenum (5,63). Gastrin cell tumors are the most common (65%), and one-third are functional (gastrinoma). Larger or periampullary lesions can cause obstruction of the duodenal ampulla and result in pancreatitis (5,6,63,88). Endoscopy and biopsy are essential to confirm the histopathologic diagnosis

**Figure 10**

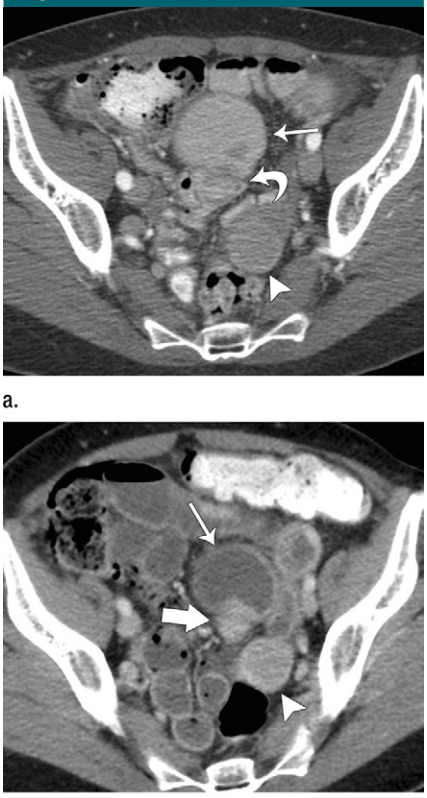

a.

b.

**Figure 10:** CT enterography in a 67-year-old woman with recurrent abdominal pain for 9 months, weight loss, and partial intermittent small-bowel occlusion. **(a)** Axial contrast-enhanced CT image obtained after positive oral contrast medium ingestion demonstrates mild dilatation of distal small bowel loop (straight arrow) without any obvious mass or wall thickening at site of transition in the ileum (curved arrow). **(b)** Axial contrast-enhanced CT enterography image obtained with neutral oral contrast medium ingestion reveals intensely enhancing mass at site of transition (thick arrow) in background of neutral oral contrast medium distending small-bowel loops (thin arrow). In the left pelvis, an incidental uterine fibroid (arrowhead in **a** and **b**) is evident. Patient underwent exploratory laparotomy and resection of approximately 90 cm of terminal ileum and right colon with evidence of multiple hard nodules in terminal ileum and lymph nodes in the mesentery. Multifocal well-differentiated carcinoid tumors with several foci of subserosal invasion were diagnosed. This case exemplifies the value of proper technique and choice of oral contrast medium to improve lesion detection.

(86) and to establish the depth of tumor infiltration in the wall and assess for regional nodal enlargement seen at

**Figure 11**

**Figure 11:** Coronal contrast-enhanced CT image in a 58-year-old man with diverticulitis, intermittent diarrhea, and occasional facial flushing shows 2.3-cm mesenteric mass with foci of calcification (arrow) in right upper quadrant, associated with intense desmoplastic reaction (arrowhead). Serum levels of 5-hydroxyindoleacetic acid, the main metabolite of serotonin, were markedly elevated. Laparoscopic right hemicolectomy yielded invasive neuroendocrine carcinoma in distal ileum (2 cm), with perineural and lymphovascular invasion and regional metastatic mesenteric nodules.

endoscopic US (63). These tumors are often difficult to detect with CT and MR imaging because of their location (40% intramural, 50% intraluminal) and small size (mostly 1–2 cm) (5,6,88). Unlike adenocarcinomas, they appear as small hypervascular intraluminal polyps or intramural lesions (6,88,91). Despite their small size, duodenal NETs can manifest with lymph node metastases in 11%–50% of cases (up to 90% in functioning gastrinomas) (5,6,63,92), whereas liver metastases occur late (5).

Ileal NETs are usually sporadic and multiple in 26%–30% of cases (63). Hepatic metastases are present at the time of diagnosis in 20% of cases (5,6,15). The common presentation is indolent and nonspecific (vague pain, bleeding, intermittent partial bowel obstruction) (6). The classic carcinoid syndrome is present in 6%–30% of patients, is associated with hepatic metastases in more than 95% of cases, and is due to the release of vasoactive compounds into the systemic circulation. Rarely this syndrome occurs if there is a direct retroperitoneal involvement, with venous drainage bypassing the liver (6,26,63). In patients suspected of having this condition, contrast-enhanced CT or MR imaging are often the preferred imaging tests, and small-bowel distention for a focused CT or MR enterography or enteroclysis examination is desirable to improve lesion detection (Fig 10) (93). These tumors manifest as a small, hypervascular, polypoid mass or as asymmetric or concentric bowel wall thickening.

Often, the secondary features, such as desmoplastic reaction in the mesentery and lymphadenopathy with or without calcification, are more easily recognized on CT and MR images than the primary lesion in the neighboring small-bowel (Fig 11). Infrequently, the patient can present with bowel obstruction or intussusception or loop ischemia or infarction due to extensive desmoplastic response that compromises the bowel lumen or mesenteric circulation (5,88).

A difficult differential diagnostic consideration in these patients with regard to CT and MR is chronic mesenteric panniculitis (also known as sclerosing mesenteritis). This entity shares some morphologic features of desmoplastic response in the small-bowel mesentery, and a tissue diagnosis of the mesenteric mass can also be difficult due to extensive fibrosis inherent to both desmoid tumors and mesenteric panniculitis. Desmoid tumors and mesenteric metastases can also uncommonly pose a diagnostic dilemma (94). Recent imaging series (39,95,96) in which the role of CT enterography and MR enteroclysis in small-bowel neoplasms (including NETs) were evaluated have shown improved sensitivity (100% and 86%–94%, respectively) and specificity (96.2% and 95%–98%, respectively) for tumor detection. Double-balloon enteroscopy and capsule endoscopy can be used to localize small NETs but have a low diagnostic yield of 33% and 45%, respectively, for primary ileal NETs (66,97). Small midgut tumors are most difficult to diagnose on the commonly used noninvasive and imaging

studies; as a result, functional SRS imaging is considered in these patients, with a reported overall sensitivity of 80–90% for octreotide scintigraphy (98). Furthermore, according to the most recent guidelines (26), all patients with midgut NETs (even without liver metastases) and those with carcinoid syndrome and suspicious symptoms (mostly, tricuspid regurgitation due to fibrosis) should undergo echocardiography to exclude carcinoid heart disease (63,93).

The appendix is the site of GEP-NETs in about 20% of cases, and up to 70% of such lesions are discovered at appendectomy performed for possible appendicitis. These lesions are small (<1 cm) and are, therefore, rarely diagnosed prospectively on the basis of imaging findings in patients suspected of having appendicitis (5,99,100). NETs in the appendix have the most favorable prognosis owing to their more indolent biology, and the risk of tumor recurrence or metastases is uncommon for small tumors (5,6,100).

Colon NETs, although rare, are typically poorly differentiated, are large (5 cm) (5), behave like adenocarcinomas, and are, therefore, managed in a similar fashion to colonic adenocarcinoma (14,24,101). The incidence of rectal carcinoids has increased over the past 3 decades (21%–27% of all GEP-NETs) (5,6,101), and the majority are incidentally detected at endoscopic evaluation to screen for colorectal cancer (7) or for other indications (50%). Infrequently, they manifest with rectal symptoms of bleeding or pain (101). Approximately 80% of rectal lesions are localized, and patients have a high survival rate (1,14). Endoscopic US is ideally suited to evaluate the depth of tumor invasion in the rectal wall (102) and to evaluate regional lymph node involvement (103). MR imaging is increasingly used to evaluate for tumor extension and node involvement, as it is for rectal adenocarcinoma. Indeed, technical developments allow the acquisition of images with high spatial resolution and thin sections, useful for adequate local staging.

In patients with colorectal NETs larger than 2 cm or those showing invasion into or beyond the rectal wall on endoscopic US or MR images, the spread of disease to other organs should be ruled out by using contrast-enhanced CT. Although, SRS can ascertain if SSRT-expressing metastases are present and guide treatment selection (101), they are not routinely recommended in rectal NETs smaller than 2 cm without invasion of the muscularis propria due to the exceptionally low risk of metastases (2% vs 48% if muscularis is invaded) (5,101).

Despite the advances in the diagnostic approaches, 20%–50% of primary NETs are difficult to localize (18), and the diagnosis is based on the histologic analysis of metastatic lesions (10). Moreover, there is no single imaging test that fulfills all the clinical expectations in evaluation of primary NETs (Table 5). Therefore, a multimodal diagnostic approach that combines both noninvasive and invasive techniques is often required in the evaluation and care of patients with GEP-NETs (18).

## Detection of Unknown Primary NETs

In patients who present with metastatic carcinoma from an unknown primary, adenocarcinomas or undifferentiated tumors are responsible in the majority of cases, followed by melanomas and squamous cell carcinomas (104). However, 11%–14% of such patients can have an NET, more commonly of low grade (Fig 12) (7,104,105). Although these patients have a poor prognosis, detection of the primary tumor site can prolong survival by about 1–2 years (104). Initial biopsy findings of the metastatic site can suggest the diagnosis of NET. Although the site of primary NET cannot routinely be ascertained from the tissue, new specific markers (ie, CDX2, PDX1, Isl1, TTF1) are now available to indicate the potential primary site (29,106–110).

The typical location of these tumors is in the gastrointestinal tract; therefore, the diagnostic investigations and imaging efforts should focus on those sites of tumor origin. However, the successful detection of primary GEP-NETs with imaging has been less than desirable (87). Studies (87,110) have reported low tumor detection sensitivities of 0%–22% for multidetector CT, 50% for CT enteroclysis, and 38%–45% for capsule endoscopy. In another study, $^{68}$Ga-DOTA-NOC PET/CT could enable detection of occult primary sites in the abdomen in 59% patients, as compared with 39% for SRS and only 20% for multidetector CT (104). Nevertheless, there are no clear recommendations for the best strategies to identify the primary tumor in patients with liver metastases from an NET (87,104). It is more practical to perform contrast-enhanced CT and SRS first to identify the primary tumor and to assess the extent of metastatic disease, as well as in patients in whom the primary tumor remains undetected (87). Surgical exploration is generally undertaken to look for primary sites in the small intestine. Studies have reported 77%–86% success in tumor localization with surgery (87,111).

## Imaging in Metastatic Disease

All NETs are potentially malignant, but the poorly differentiated ones exhibit more aggressive behavior (6,18). Regional and distant disease spread are reported in 20%–40% of cases (7). Nonfunctioning tumors of the pancreas and gastrointestinal tract are more likely to metastasize (6,112). The most common metastatic sites are lymph nodes and liver, followed by lungs, bones (7%–15%), peritoneum and mesentery (6%, mostly in ileal carcinoids), soft tissue, brain (1.5%), and breast (113–115).

In NETs of the small bowel, a correlation between the size of primary tumor and the probability of metastasis has been shown, with metastases present in 15%–25% of patients with primary tumor diameter smaller than 1 cm, in 58%–80% of patients with tumor diameter of 1–2 cm, and in more than 75% of patients with tumor diameter larger than 2 cm (38,104). In patients with liver metastases and carcinoid syndrome, Cushing syndrome and carcinoid heart disease are present in up to 20% of cases (63,112,116). Moreover, the presence of liver metastases is the single most important factor that

**Table 5**

**Morphologic and Functional Imaging and Invasive Techniques for GEP-NETs**

| Site | Multidetector CT* | MR Imaging† | SRS‡ | FDG PET§ | Endocsopic US or Endoscopy‖ |
|---|---|---|---|---|---|
| Pancreatic | | | | | Detection of small lesions, particularly < 2 cm (62,67,86); endoscopic US–guided fine-needle aspiration for histopathologic evaluation |
| Functional | Small (1–2 cm), well defined, hypervascular | Additional features: T2 hyperintense, T1 hypointense | Insulinomas: low expression of SSTR (50%–60%) (22,38,73) | | Best modality for small tumor detection (67) |
| Nonfunctional | Large (~ 4 cm) capsulated, heterogeneous enhancement; necrotic or cystic changes are common, occasionally purely cystic; calcifications in malignant tumors; local invasion and metastases (up to 80% of cases) (6) | Additional features: T2 hyperintense, T1 hypointense | Problem solving | | Tissue diagnosis in incidental lesions |
| Performance (%) | 69–80 (43,69–73) | 74–94 (43,69,81) | Insulinomas: 14–53; nonfunctioning, gastrinomas, glucagonomas: 75–100 (16,38,49,73) | | 84.2–91.7 (67) |
| Metastases | Liver is the common site; arterially enhancing with washout on late phase; sensitivity, 82%–100% (11,120) | Additional features: T2 hyperintense, T1 iso- to hypointense; Sensitivity, 55%–79% (10,120) | Sensitivity, 81%–96% (4,11,117,120,126) | Evaluation of posttreatment dedifferentiation | Restricted field of view; possible endoscopic US–guided fine-needle aspiration |
| Extrapancreatic | | | | | |
| Stomach | Types I and II are enhancing polypoid or submucosal lesions <2 cm; larger lesions may have uclerations; CT might miss lesions <1 cm; CT and double-contrast radiography yield findings similar to those of other submucosal or polypoid lesions; type III are large (>2 cm) with infiltrative morphology (malignant) and may be ulcerated | | | | Gastroscopy to localize lesion; findings similar to those of other submucosal or polypoid lesions; endoscopic US for evaluation of depth of tumor invasion in wall and biopsy |
| Duodenum | Generally small (1–2 cm), arterial phase enhancing lesion; possible ulceration; 50%: intraluminal polyps; 40%: intramural mass; possible obstructive biliary dilatation (large or periampullary lesions) | Additional features: T2 hyperintense, T1 hypointense | | | Detection of small lesions, particularly <2 cm (62,67,86); endoscopic US–guided fine-needle aspiration for histopathologic evaluation |

Table 5 (continues)

**Table 5 (continued)**

**Morphologic and Functional Imaging and Invasive Techniques for GEP-NETs**

| Site | Multidetector CT* | MR Imaging† | SRS‡ | FDG PET§ | Endocsopic US or Endoscopy‖ |
|---|---|---|---|---|---|
| Small bowel | Hypervascular lesion (intraluminal/intramural) or bowel thickening; additional findings: desmoplastic reaction (mesentery), mesenteric masses with or without calcification; calcification in 70% of mesenteric node metastases; complications: bowel obstruction, loop ischemia/infarction; sensitivity of CT enterography: 100% (39) | Additional features: T2 hyperintense, T1 hypointense; best visualized on gadolinium-enhanced T1-weighted MR images with fat suppression; sensitivity of MR enteroclysis: 86%–94% (96,97) | 80%–90% (98) | | Possible endoscopic US evaluation of terminal ileum (miniprobes through biopsy channel of colonoscope); other techniques include double-balloon enteroscopy and capsule endoscopy (diagnostic yield, 33% and 45%, respectively) (67,98) |
| Appendix | Generally small (<1cm) enhancing lesions; diffuse circumferential mural thickening; possible associated findings of appendicitis (primary tumor may not be readily seen) | | | | |
| Colon | Commonly large (~5 cm) ulcerating lesions (more common in ascending [right] colon) or necrotic; risk of colocolonic intussusceptions, bowel obstruction | | | | Colonoscopy: localization and biopsy |
| Rectum | Generally small (< 1 cm) submucosal lesions | | | | Endoscopy: small solitary nodule or polypoid mass; endoscopic US for evaluation of depth of tumor invasion in wall and biopsy guidance |
| Metastases | Same as for pancreas | Same as for pancreas | Same as for pancreas | Same as for pancreas | Same as for pancreas |

Note.—Numbers in parentheses are references.

* Advantages include faster acquisition, superior spatial resolution, and multiplanar display.

† Advantages include focused examination, superior soft-tissue contrast; ability to depict and characterize small lesions in pancreas and liver.

‡ Advantages include sensitivity for lesions expressing SSTRs and ability to evaluate patients for biologic therapies.

§ Advantages include ability to demonstrate malignant and poorly differentiated tumors.

‖ Advantages include ability to demonstrate small tumors and to guide biopsy.

influences patient survival and prognosis (104). The number of metastases appears to further affect survival (117,118). Liver failure is the most common cause of death, followed by bowel obstruction and ischemia (24).

All available imaging modalities frequently miss small (<0.5-cm) liver metastases (10,119). Studies on US for detection of liver metastases in NETs are scarce: The sensitivity is reported as variable (14%–88%) (10,11,120), while specificity is higher (92%–100%) (11,120). On multiphasic contrast-enhanced CT or MR images, hepatic lesions are usually hypervascular in the arterial phase and demonstrate washout in the late phase (~70% of cases) (38,112,118,121). Less frequently, they show a hypovascular pattern (15%) or a progressive fill in that mimics hemangioma (10%) (121). Multidetector CT has a reported mean sensitivity of 82%–100% and specificity of 83%–100% (11,120). On unenhanced MR images, liver metastases are generally iso- to hypointense on T1-weighted images and moderately to strongly hyperintense on T2-weighted images. In particular, T2-weighted fast spin-echo images with fat suppression (high contrast

**Figure 12**

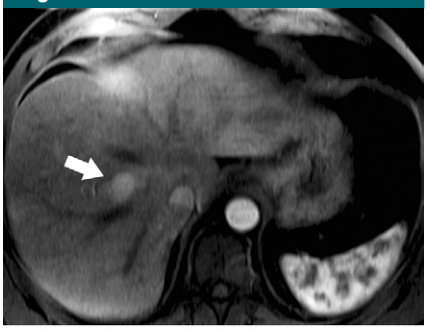

a.

b.

**Figure 12:** Images in a 48-year-old man with known Crohn disease. An indeterminate liver lesion was incidentally detected on contrast-enhanced CT study of the abdomen (not shown); no other abnormalities were present. **(a)** Axial arterial phase contrast-enhanced MR image (4.63/2.26; flip angle, 90°) shows single arterially enhancing lesion (arrow) in VIII segment. CT-guided biopsy of the lesion led to diagnosis of metastatic NET of intestinal origin (positive for CDX-2 at immunohistochemical analysis). **(b)** Coronal venous phase contrast-enhanced CT enterography, performed to evaluate small bowel, shows 2-cm enhancing mass (arrow) in distal ileum. Patient underwent surgical resection of the ileum, confirming diagnosis of a low-grade (G1; Ki-67 index < 2%) NET. Radiofrequency ablation of the hepatic lesion was performed.

**Figure 13**

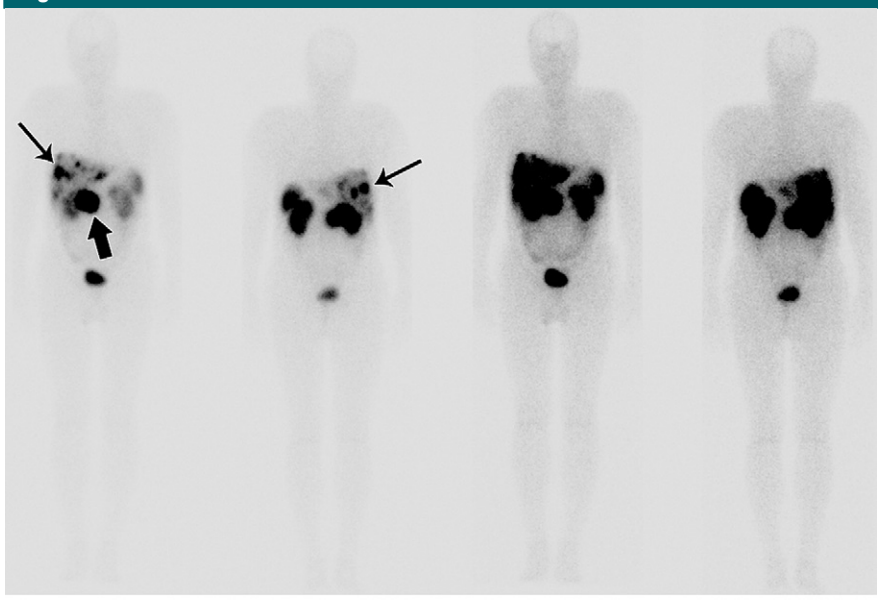

a.

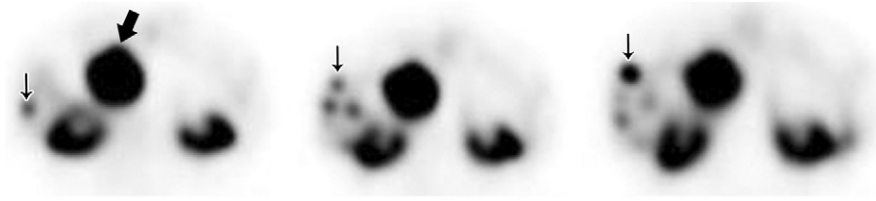

b.

**Figure 13:** Metastatic well-differentiated pancreatic NET in a 57-year-old man. **(a)** Octreotide whole-body scans and **(b)** axial SPECT images obtained 24 hours after injection of 185 MBq $^{111}$In pentetreotide show multiple foci of increased radiotracer uptake in liver (thin arrows). Another large focus of radiotracer uptake is seen in the epigastrium, just to the right of midline (thick arrow), consistent with a mass in the head of the pancreas found on prior CT images (not shown), and **b** helps correctly distinguish between physiologic renal excretion of radiotracer (posterior) and pancreatic mass (anterior).

between lesion and liver) and early arterial phase contrast-enhanced T1-weighted images have been shown to be the most sensitive for detection of liver metastases of endocrine origin (112,118,121). The overall mean detection rate for MR imaging is 80%–85% (11), the sensitivity is 55%–79% (10,120), and the specificity is 88%–100% (120). The use of diffusion-weighted imaging and ADCs can improve the detection and characterization ability of MR imaging for malignant liver lesions (122,123). In a recent study (124), liver metastases from NETs had significantly lower ADCs than did those of benign hepatic lesions.

Functional imaging plays a crucial role in the evaluation of metastatic NETs. Despite low spatial resolution, SRS has a reported high sensitivity (81%–96%) and specificity (up to 88%) for detection of liver metastases (4,11,117,118,120,125). However, detection rates reported in the literature are discordant: According to different authors, SRS can enable detection of more hepatic lesions per patient than other imaging studies (10,117,120). However, in a study published by Dromain et al (118) in 2005, MR imaging depicted a far greater number of liver metastases. The additional value of SRS is related to its ability in helping evaluate the SSTR status of the lesions (55), and in 20%–55% of patients SRS findings can substantially affect therapy management (117,126). Therefore, primary NETs or metastatic lesions with high SSTR concentrations are suitable for therapy with somatostatin analogs or for peptide receptor radionuclide treatment (Fig 13). $^{68}$Ga-DOTATOC PET

**Figure 14**

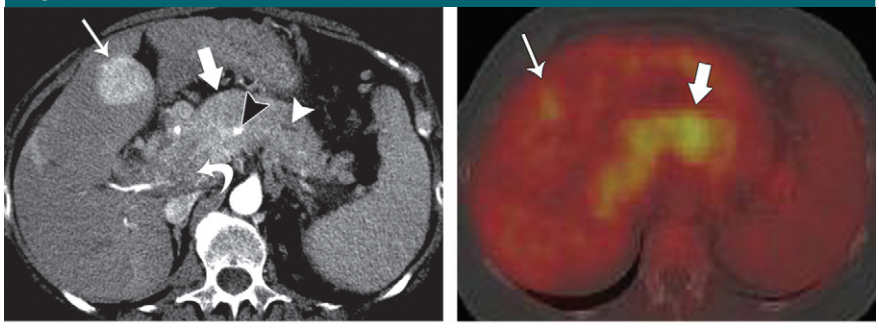

a. b.

**Figure 14:** Images in a 61-year-old woman who presented with 2 weeks of gastroesophageal reflux symptoms, abdominal pain, and diarrhea. **(a)** Axial early arterial phase contrast-enhanced CT image shows infiltrating enhancing mass in pancreatic head and body (thick arrow) causing dilatation of main pancreatic duct (white arrowhead), encasing the splenic artery (black arrowhead), and invading the portal vein (curved arrow). Two metastases in the liver are also seen, in segment IV (thin arrow) and segment VII (not shown). **(b)** Corresponding fused FDG PET/CT image shows obvious radiotracer uptake in pancreatic mass (thick arrow) and moderate uptake in liver lesion (thin arrow). Biopsy of the liver yielded diagnosis of well-differentiated metastatic NET.

can depict additional sites of metastatic spread (10,127), but, again, $^{68}$Ga generators are not widely available (10).

The prevalence of nodal metastases from small-bowel NETs is related to primary tumor size: 20%–30% for tumors smaller than 1 cm, 60%–80% for lesions 1–2 cm, and 80% for tumors larger than 2 cm (38). The morphologic criteria (short-axis diameter > 1 cm, rounded shape) used are not accurate enough to enable evaluation of nodal involvement. Although only a few investigators have studied the value of imaging for nodal metastases from NETs, the role of functional techniques is predictable, according to results achieved for other neoplasms (128,129). In a study performed by Prasad et al (104) $^{68}$Ga-DOTANOC PET helped identify lymph node involvement in all patients, whereas CT helped identify nodal involvement in only 50%. For bone metastases, SRS showed a variable sensitivity (50%–70%), compared with bone scans (90%–100%) and MR imaging (100%) (120). Recently, $^{68}$Ga-DOTATOC PET has demonstrated high sensitivity (97%) and specificity (92%) for early detection of bone metastases (130). Poorly differentiated tumors with a high proliferation index tend to scarcely express SSTR and are typically FDG positive. Therefore FDG PET and PET/CT are strong prognostic markers, allowing identification of NETs characterized by aggressive growth or increased propensity for invasion and metastasis (Fig 14) (3,48,49,57–59).

## Treatment

Complete surgical resection is the first-line and potentially curative treatment of primary GEP-NETs, regardless of their origin (86). The surgical approach, however, is influenced by lesion size and location, disease stage, and the patient's symptoms. Limited resection is considered when the lesion is noninvasive and small in size (<2 cm): small insulinomas (131), type I or II gastric carcinoids, small duodenal lesions, and noninvasive rectal (132) and appendiceal tumors (100). However, radical surgery (generally laparotomy) along with resection of draining lymph nodes is instead recommended for small-bowel NETs (often small and multiple), MEN-1 patients with duodenal and/or pancreatic lesions larger than 2 cm (often multiple), nonfunctioning NETs (usually malignant), type III gastric carcinoids (gastrectomy), cecal and colonic tumors (behave more like adenocarcinoma counterpart), rectal NETs larger than 2.5 cm or invasive (14,24,131), and invasive large (>2-cm) or base-located appendiceal carcinoids along with right hemicolectomy (24,100).

Even when liver metastases are present, surgery can be curative, with a 5-year survival rate of up to 60%–80% (133). Partial hepatic resection can be performed concurrently with the primary tumor removal (86). Liver resection is generally not considered in patients with multifocal liver disease or in those with extrahepatic spread (133). Nevertheless in selected, generally young, patients, two-step resection and cytoreductive surgery have been proposed (133,134). Liver transplantation as a therapeutic option is feasible in selected patients with unresectable metastatic NETs (Milan criteria) (24,135). A surgical approach with a palliative aim is also often used to treat pain, as well as complications such as bleeding, perforation, or obstruction, even in metastatic disease (24). In patients with symptoms due to increased hormone secretion from metastatic disease who are deemed ineligible for resection, local-regional cytoreductive therapies such as radiofrequency ablation embolization techniques (bland embolization or transarterial chemoembolization) and radioembolization have been successfully applied to control symptoms or tumor burden (35%–90%) (86,133,136,137). Moreover, cytoreductive ablative therapies, in addition to surgical resection, can offer improved survival and quality of life at 5 years as compared with patients who do not undergo surgery (70%–90% vs 50%) (24).

A variety of medical treatments are available for NETs, but few have been the subject of well-designed controlled trials (136). Biologic treatment with somatostatin analogs (octreotide, lanreotide) and receptor-targeted radionuclide agents are available for tumors that expressing SSTRs. Patients whose tumors are well-differentiated or who have low-proliferation-index primary tumors or metastases are the most suitable candidates for treatment with these agents (136,138,139). The extent of SSTR expression can also serve as a predictive marker of better treatment response

(54,140,141). Somatostatin analogs can produce an antiproliferative effect (8,138,142) and control systemic symptoms in patients with functional lesions or metastatic NETs and in those with carcinoid syndrome (136,138). Interferon-α can be combined with somatostatin analogs and reduce symptoms in 30%–70% of cases (mostly nonfunctioning pancreatic NETs or slow-growing tumors or in patients with disseminated disease) and in some studies has shown tumor response or stabilization in up to 70% of patients (86,133,136). Receptor-targeted radionuclide agents are being investigated as additional therapeutic options in symptomatic patients with liver metastases (133), but their availability is limited to only a few specialist centers (136).

In patients with aggressive tumor biology (highly proliferative and/or poorly differentiated) or metastatic lesions without uptake on SRS images, systemic chemotherapy can be considered (86,136,143). Even without prolonged remission (median of 6 months), cytotoxic chemotherapy can produce a response rate of 42%–67% for highly proliferative NETs (Ki-67 index > 20%). On the other hand, a low index of proliferation (Ki-67 index < 2%) tends to suggest resistance to chemotherapy; therefore, the role of cytotoxic agents in well-differentiated tumors is limited (response rate < 15%) (8,24,136,139,143). For patients in whom other therapies have failed, new drugs that target tumor angiogenesis (bevacizumab, everolimus, sunitinib) are being investigated in clinical trials. Although encouraging antitumor activity has been shown, data on patient survival are not clear. Therefore the role of these antiangiogenesis agents is not yet established in treating NETs (133,136,138,144,145).

## Follow-up

The follow-up approach is related to tumor status at time of diagnosis and disease stage, which directly affect length of survival (26). Further investigations are not routinely indicated after curative resection for a small (<2-cm) sporadic insulinoma, appendiceal tumors smaller than 1 cm diagnosed at appendectomy, and endoscopically resectable benign (<2-cm noninvasive NETs) rectal and type I gastric NETs (21,100,146). However, follow-up is required for more aggressive lesions: nonfunctioning pancreatic tumors or tumors larger than 2 cm (24), type III gastric lesions (21), invasive appendiceal tumors that are larger than 2 cm, ileal and colonic NETs (146) and those with metastatic disease.

Follow-up for NETs requires a multidisciplinary approach, including biochemical (chromogranin A, hormones, vasoactive amines), radiologic, and histologic investigations (146). The imaging modality of choice should be that which best demonstrated the tumor at diagnosis. Thus, SSTR imaging is recommended for tumors known to be SSTR-positive, while follow-up for SSTR-negative NETs should rely on multidetector CT or MR imaging (26).

Contrast-enhanced CT or MR imaging plays a central role in long-term assessment after surgery. The follow-up protocol includes imaging studies every 6 months for the 1st year and then at yearly intervals if negative (Fig 15). The follow-up interval is shorter (3 months) for intermediate- and high-grade lesions (146) and in patients undergoing chemotherapy or biologic therapies (8). The evaluation of response to treatment on CT mostly relies on the changes in tumor burden (38,139).

Octreotide scintigraphy can be used for prediction of response to targeted therapies in lesions that are positive on SRS images at time of diagnosis (38,139). A lesion that is negative on SRS images after treatment may indicate either complete remission or heterogeneity of the lesion due to necrosis, such as in subsequent tumor dedifferentiation, which is associated with a worse prognosis (139). Nevertheless, the role of routine octreotide scintigraphy in follow-up has still not been defined (98). SRS is generally required every 2 years (or 12 months in more aggressive [G2 or G3] lesions) or when a new lesion appears on CT or MR images (146). An additional role can be played by FDG PET. Because FDG PET primarily helps identify poorly differentiated tumors, dual tracer imaging (with both somatostatin analogs and FDG) might possibly be useful in posttherapy assessment to evaluate for eventual tumor dedifferentiation (3,139).

Other imaging biomarkers such as diffusion-weighted and perfusion

**Figure 15**

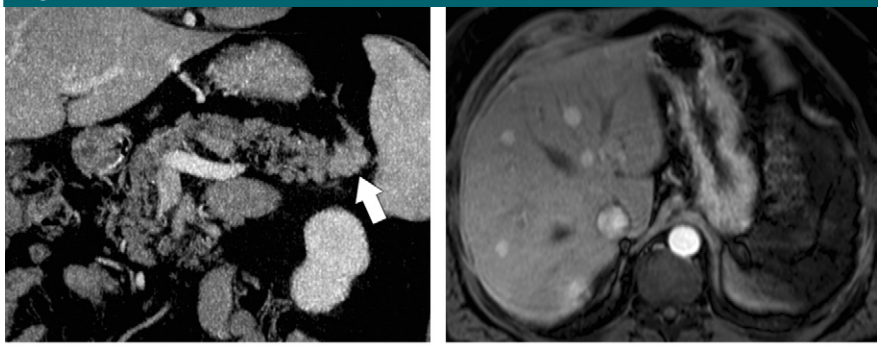

a. b.

**Figure 15:** Recurrence of small nonfunctioning pancreatic NET in a 66-year-old woman with microscopic hematuria. **(a)** Coronal venous phase contrast-enhanced CT image from the hematuria protocol CT shows 2.5-cm solid enhancing lesion in pancreatic tail (arrow). Differential diagnosis of intrapancreatic splenule was entertained, along with incidental NET as a possibility. Sulfur colloid scintigram (not shown) was negative for splenic tissue in the pancreas. Laparoscopic distal pancreatectomy and splenectomy resulted in diagnosis of well-differentiated pancreatic NET with moderate mitotic activity (three mitoses per 10 high-power fields). Four months after surgery, follow-up contrast-enhanced CT image (not shown) showed liver lesions. **(b)** Axial arterial phase contrast-enhance MR image (5.11/2.3; flip angle, 10°) obtained for evaluation of hepatic lesions shows multiple arterially enhancing liver lesions. CT-guided biopsy revealed metastatic pancreatic NET.

**Figure 16**

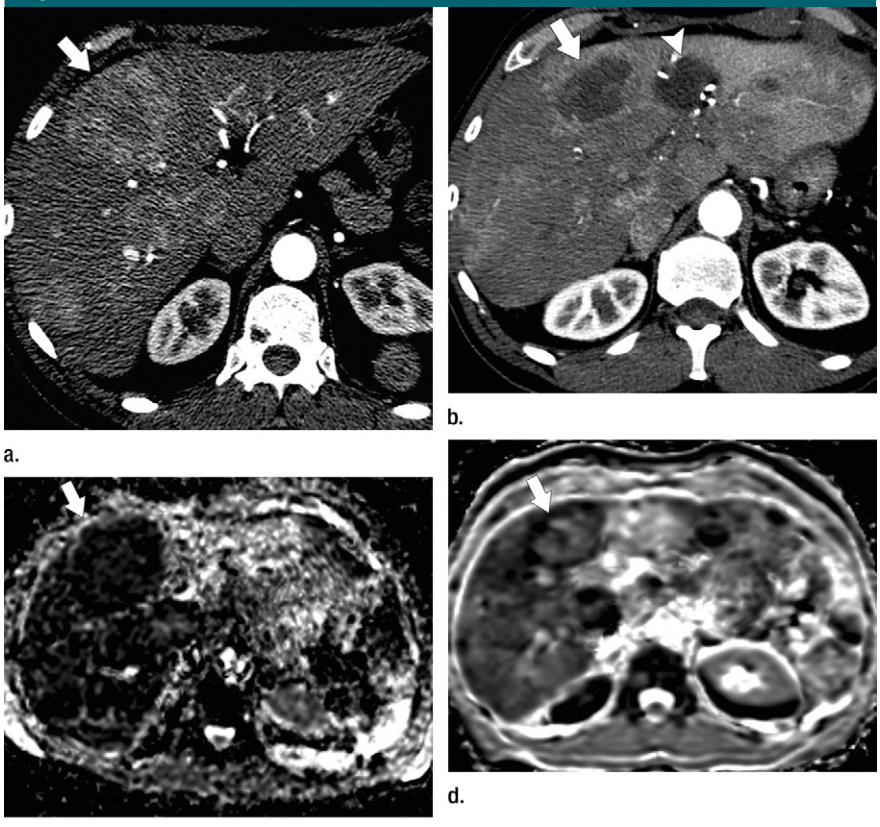


**Figure 16:** Metastatic ileal carcinoid in a 54 year-old-man. Axial arterial phase contrast-enhanced CT image obtained **(a)** before treatment with somatostatin analogs shows enhancing heterogeneous mass (arrow) in right lobe of the liver. **(b)** On axial arterial phase contrast-enhanced CT image obtained 1 year after therapy, the mass has a large necrotic component, with reduced tumor viability and partial shrinkage (arrow). Also, a hypoattenuating area (arrowhead) adjacent to the main lesion is related to a postoperative collection. **(c, d)** On ADC maps obtained **(c)** before ($b$ = 0 sec/mm$^2$; 3000/83.6; flip angle, 90°) and **(d)** after treatment (b = 600 sec/mm$^2$; 3000/65.4; flip angle, 90°) on the same day of CT the tumor show restricted diffusion on **c** (arrow) and increased signal intensity on **d** (arrow), which is related to treatment-induced necrosis in the metastatic lesion.

imaging are being evaluated to assess effectiveness of organ-directed treatment within weeks of initiating therapy (Fig 16). An increase in tumor ADC after transarterial chemoembolization correlates with a response to therapy (147). Similarly, CT perfusion can be used to evaluate response to antiangiogenetic drugs (eg, bevacizumab) as early as 48 hours after initiation of therapy (38).

## Screening in High-Risk Patients with Genetic Defects

According to the most recent guidelines (26), clinical examination to exclude complex cancer syndromes (eg, MEN-1) should be performed and a family history taken in all cases of NET. In asymptomatic patients with MEN-1, family members should undergo regular surveillance for early tumor detection. The typical protocol for MEN-1 includes clinical and biochemical (serum calcium, parathyroid hormone, chromogranin A) evaluations every 6–12 months and imaging after age 15 years with MR (head and abdomen) and multidetector CT (chest), repeated every 2–5 years (9,23). Endoscopic US and MR imaging are considered complementary for assessing pancreatic tumors in patients with MEN-1 (148). In patients with Von Hippel–Lindau disease, screening should start from infancy or early childhood and include annual retinal examination, laboratory analysis (catecholamines), and imaging of the kidneys (abdominal US; MR imaging after age 20 years or if the US findings are abnormal), pancreas, adrenals (starting when the patient is an adolescent), brain, and spine (MR imaging, starting when the patient is 10 years old) (9). In cases of neurofibromatosis type 1 clinical evaluation (blood pressure, skin, growth measurements, skeletal changes, precocious puberty), an annual ophthalmologic examination (for optic gliomas) and patient education appear to be helpful in detecting complications and are considered adequate (9,149). Specific recommendations for surveillance of endocrine tumors (somatostinoma, pheochromocytoma) do not exist (22). Baseline imaging studies (brain and spine MR imaging, conventional radiographs of bones, evaluation of chest and abdomen) do not seem to influence management, and their role depends on the history and physical findings (9,149). In children with tuberous sclerosis complex, brain MR imaging, renal US, and an electrocardiogram are indicated at presentation. Practice guidelines for surveillance of NETs (pituitary, parathyroid, and pancreatic) have not been developed, and screening for these entities is not included in current recommendations. Specific imaging studies should be required, depending on symptoms suggestive of NET. Resection is reported as the first line of treatment for pancreatic tumors in patients with Von Hippel–Lindau disease (22) and in patients with MEN-1 (24). Follow up investigations must be individualized according to size and growth behavior of individual tumors, but imaging intervals (CT, MR) are generally between 1 and 2 years (146).

## Conclusions

GEP-NETs are a heterogeneous and complex group of neoplasms with a wide spectrum of clinical manifestations, although currently they are more

frequently detected with imaging or endoscopic studies. The histologic diagnosis of GEP-NETs relies on the demonstration of neuroendocrine markers in the tissue, and, depending on the clinical manifestation, several serum and urine markers can be tested. Imaging strongly contributes in patient care, and its role mostly involves detection and characterization of the primary lesions, staging, and subsequent follow-up. Morphologic imaging, such as multidetector CT and MR imaging are the most widely used techniques for the initial evaluation and for exclusion of metastatic disease. The role of functional imaging (SRS, PET) is related to the increased expression of somatostatin receptors at the cell membrane. The extent of SSTR expression at the time of diagnosis is useful as a prognostic indicator and can affect clinical management, indicating the potential for treatment with targeted therapies, which represent an alternative to surgery, the only potentially curative treatment. Both morphologic and functional imaging techniques play a complementary role, directed mainly by tumor status at time of presentation.

**Disclosures of Conflicts of Interest: D.V.S.** Financial activities related to the present article: none to disclose. Financial activities not related to the present article: institution has grants or grants pending from GE Healthcare; author receives royalties from Elsevier. Other relationships: none to disclose. **P.A.B.** No relevant conflicts of interest to disclose. **C.F.** No relevant conflicts of interest to disclose. **M.A.B.** Financial activities related to the present article: none to disclose. Financial activities not related to the present article: receives royalties from Springer. Other relationships: none to disclose.

## References

1. Lawrence B, Gustafsson BI, Chan A, Svejda B, Kidd M, Modlin IM. The epidemiology of gastroenteropancreatic neuroendocrine tumors. Endocrinol Metab Clin North Am 2011;40(1):1–18, vii.
2. Rindi G. The ENETS guidelines: the new TNM classification system. Tumori 2010;96(5):806–809.
3. Tan EH, Tan CH. Imaging of gastroenteropancreatic neuroendocrine tumors. World J Clin Oncol 2011;2(1):28–43.
4. Turaga KK, Kvols LK. Recent progress in the understanding, diagnosis, and treatment of gastroenteropancreatic neuroendocrine tumors. CA Cancer J Clin 2011;61(2):113–132.
5. Chang S, Choi D, Lee SJ, et al. Neuroendocrine neoplasms of the gastrointestinal tract: classification, pathologic basis, and imaging features. RadioGraphics 2007;27(6):1667–1679.
6. Heller MT, Shah AB. Imaging of neuroendocrine tumors. Radiol Clin North Am 2011;49(3):529–548, vii.
7. Yao JC, Hassan M, Phan A, et al. One hundred years after "carcinoid": epidemiology of and prognostic factors for neuroendocrine tumors in 35,825 cases in the United States. J Clin Oncol 2008;26(18):3063–3072.
8. Oberg K, Akerström G, Rindi G, Jelic S; ESMO Guidelines Working Group. Neuroendocrine gastroenteropancreatic tumours: ESMO Clinical Practice Guidelines for diagnosis, treatment and follow-up. Ann Oncol 2010;21(Suppl 5):v223–v227.
9. Toumpanakis CG, Caplin ME. Molecular genetics of gastroenteropancreatic neuroendocrine tumors. Am J Gastroenterol 2008;103(3):729–732.
10. Modlin IM, Oberg K, Chung DC, et al. Gastroenteropancreatic neuroendocrine tumours. Lancet Oncol 2008;9(1):61–72.
11. Sundin A, Vullierme MP, Kaltsas G, Plöckinger U; Mallorca Consensus Conference participants; European Neuroendocrine Tumor Society. ENETS Consensus Guidelines for the Standards of Care in Neuroendocrine Tumors: radiological examinations. Neuroendocrinology 2009;90(2):167–183.
12. Ito T, Sasano H, Tanaka M, et al. Epidemiological study of gastroenteropancreatic neuroendocrine tumors in Japan. J Gastroenterol 2010;45(2):234–243.
13. Modlin I, Zikusoka M, Kidd M, Latich I, Eick G, Romanyshyn J. The history and epidemiology of neuroendocrine tumours. In: Handbook of neuroendocrine tumours. Bristol, England: BioScientifica, 2006; 7–37.
14. Modlin IM, Lye KD, Kidd M. A 5-decade analysis of 13,715 carcinoid tumors. Cancer 2003;97(4):934–959.
15. Modlin IM, Sandor A. An analysis of 8305 cases of carcinoid tumors. Cancer 1997;79(4):813–829.
16. Oberg K. Pancreatic endocrine tumors. Semin Oncol 2010;37(6):594–618.
17. Klöppel G, Couvelard A, Perren A, et al. ENETS Consensus Guidelines for the Standards of Care in Neuroendocrine Tumors: towards a standardized approach to the diagnosis of gastroenteropancreatic neuroendocrine tumors and their prognostic stratification. Neuroendocrinology 2009;90(2):162–166.
18. Schott M, Klöppel G, Raffel A, Saleh A, Knoefel WT, Scherbaum WA. Neuroendocrine neoplasms of the gastrointestinal tract. Dtsch Arztebl Int 2011;108(18):305–312.
19. Hassan MM, Phan A, Li D, Dagohoy CG, Leary C, Yao JC. Risk factors associated with neuroendocrine tumors: A U.S.-based case-control study. Int J Cancer 2008;123(4):867–873.
20. Nascimbeni R, Villanacci V, Di Fabio F, Gavazzi E, Fellegara G, Rindi G. Solitary microcarcinoid of the rectal stump in ulcerative colitis. Neuroendocrinology 2005;81(6):400–404.
21. Kulke MH, Anthony LB, Bushnell DL, et al. NANETS treatment guidelines: well-differentiated neuroendocrine tumors of the stomach and pancreas. Pancreas 2010;39(6):735–752.
22. Lodish MB, Stratakis CA. Endocrine tumours in neurofibromatosis type 1, tuberous sclerosis and related syndromes. Best Pract Res Clin Endocrinol Metab 2010;24(3):439–449.
23. Waldmann J, Fendrich V, Habbe N, et al. Screening of patients with multiple endocrine neoplasia type 1 (MEN-1): a critical analysis of its value. World J Surg 2009;33(6):1208–1218.
24. Boudreaux JP. Surgery for gastroenteropancreatic neuroendocrine tumors (GEP-NETS). Endocrinol Metab Clin North Am 2011;40(1):163–171, ix.
25. Shehata BM, Stockwell CA, Castellano-Sanchez AA, Setzer S, Schmotzer CL, Robinson H. Von Hippel-Lindau (VHL) disease: an update on the clinico-pathologic and genetic aspects. Adv Anat Pathol 2008;15(3):165–171.
26. Ramage JK, Ahmed A, Ardill J, et al. Guidelines for the management of gastroenteropancreatic neuroendocrine (including carcinoid) tumours (NETs). Gut 2012;61(1):6–32.
27. Zatelli MC, Torta M, Leon A, et al. Chromogranin A as a marker of neuroendocrine neoplasia: an Italian multicenter study. Endocr Relat Cancer 2007;14(2):473–482.
28. Modlin IM, Gustafsson BI, Moss SF, Pavel M, Tsolakis AV, Kidd M. Chromogranin A—biological function and clinical utility in neuro endocrine tumor disease. Ann Surg Oncol 2010;17(9):2427–2443.

29. Klimstra DS, Modlin IR, Coppola D, Lloyd RV, Suster S. The pathologic classification of neuroendocrine tumors: a review of nomenclature, grading, and staging systems. Pancreas 2010;39(6):707–712.

30. Lloyd RV. Practical markers used in the diagnosis of neuroendocrine tumors. Endocr Pathol 2003;14(4):293–301.

31. Solcia E, Kloppel G, Sobin LH. Histological typing of endocrine tumours. In: WHO international histological classification of tumours. 2nd ed. Berlin, Germany: Springer, 2000.

32. Rindi G, Klöppel G, Alhman H, et al. TNM staging of foregut (neuro)endocrine tumors: a consensus proposal including a grading system. Virchows Arch 2006;449(4):395–401.

33. Rindi G, Klöppel G, Couvelard A, et al. TNM staging of midgut and hindgut (neuro) endocrine tumors: a consensus proposal including a grading system. Virchows Arch 2007;451(4):757–762.

34. Hochwald SN, Zee S, Conlon KC, et al. Prognostic factors in pancreatic endocrine neoplasms: an analysis of 136 cases with a proposal for low-grade and intermediate-grade groups. J Clin Oncol 2002;20(11):2633–2642.

35. Bosman F, Carneiro F, Hruban RH, Theise N. WHO classification of tumours of the digestive system. Lyon, France: IARC Press, 2010.

36. Klimstra DS, Modlin IR, Adsay NV, et al. Pathology reporting of neuroendocrine tumors: application of the Delphic consensus process to the development of a minimum pathology data set. Am J Surg Pathol 2010;34(3):300–313.

37. Modlin IM, Gustafsson BI, Kidd M. Gastrointestinal carcinoid tumours. In: Howden CW, ????? BJ, Buchman AL, Metz DC, Modlin IM, eds. Advances in digestive disease. Bethesda, Md: AGA Institute Press, 2007.

38. Tamm EP, Kim EE, Ng CS. Imaging of neuroendocrine tumors. Hematol Oncol Clin North Am 2007;21(3):409–432, vii.

39. Kamaoui I, De-Luca V, Ficarelli S, Mennesson N, Lombard-Bohas C, Pilleul F. Value of CT enteroclysis in suspected small-bowel carcinoid tumors. AJR Am J Roentgenol 2010;194(3):629–633.

40. Dumortier J, Ratineau C, Roche C, Lombard-Bohas C, Chayvialle JA, Scoazec JY. Angiogenesis and endocrine tumors [in French]. Bull Cancer 1999;86(2):148–153.

41. Procacci C, Carbognin G, Accordini S, et al. Nonfunctioning endocrine tumors of the pancreas: possibilities of spiral CT characterization. Eur Radiol 2001;11(7):1175–1183.

42. Herwick S, Miller FH, Keppke AL. MRI of islet cell tumors of the pancreas. AJR Am J Roentgenol 2006;187(5):W472–W480.

43. Ichikawa T, Peterson MS, Federle MP, et al. Islet cell tumor of the pancreas: biphasic CT versus MR imaging in tumor detection. Radiology 2000;216(1):163–171.

44. Woodard PK, Feldman JM, Paine SS, Baker ME. Midgut carcinoid tumors: CT findings and biochemical profiles. J Comput Assist Tomogr 1995;19(3):400–405.

45. Bader TR, Semelka RC, Chiu VC, Armao DM, Woosley JT. MRI of carcinoid tumors: spectrum of appearances in the gastrointestinal tract and liver. J Magn Reson Imaging 2001;14(3):261–269.

46. Owen NJ, Sohaib SA, Peppercorn PD, et al. MRI of pancreatic neuroendocrine tumours. Br J Radiol 2001;74(886):968–973.

47. Cimitan M, Buonadonna A, Cannizzaro R, et al. Somatostatin receptor scintigraphy versus chromogranin A assay in the management of patients with neuroendocrine tumors of different types: clinical role. Ann Oncol 2003;14(7):1135–1141.

48. Kayani I, Bomanji JB, Groves A, et al. Functional imaging of neuroendocrine tumors with combined PET/CT using 68Ga-DOTATATE (DOTA-DPhe1,Tyr3-octreotate) and 18F-FDG. Cancer 2008;112(11):2447–2455.

49. Miederer M, Weber MM, Fottner C. Molecular imaging of gastroenteropancreatic neuroendocrine tumors. Gastroenterol Clin North Am 2010;39(4):923–935.

50. Oberg K. Diagnostic pathways. In: Handbook of neuroendocrine tumors. Bristol, England: BioScientifica, 2006; 101–121.

51. Taniyama Y, Suzuki T, Mikami Y, Moriya T, Satomi S, Sasano H. Systemic distribution of somatostatin receptor subtypes in human: an immunohistochemical study. Endocr J 2005;52(5):605–611.

52. Bakker WH, Krenning EP, Reubi JC, et al. In vivo application of [111In-DTPA-D-Phe1]-octreotide for detection of somatostatin receptor-positive tumors in rats. Life Sci 1991;49(22):1593–1601.

53. Ricke J, Klose KJ, Mignon M, Oberg K, Wiedenmann B. Standardisation of imaging in neuroendocrine tumours: results of a European delphi process. Eur J Radiol 2001;37(1):8–17.

54. Gibril F, Reynolds JC, Chen CC, et al. Specificity of somatostatin receptor scintigraphy: a prospective study and effects of false-positive localizations on management in patients with gastrinomas. J Nucl Med 1999;40(4):539–553.

55. Virgolini I, Ambrosini V, Bomanji JB, et al. Procedure guidelines for PET/CT tumour imaging with 68Ga-DOTA-conjugated peptides: 68Ga-DOTA-TOC, 68Ga-DOTA-NOC, 68Ga-DOTA-TATE. Eur J Nucl Med Mol Imaging 2010;37(10):2004–2010.

56. Miederer M, Seidl S, Buck A, et al. Correlation of immunohistopathological expression of somatostatin receptor 2 with standardised uptake values in 68Ga-DOTA-TOC PET/CT. Eur J Nucl Med Mol Imaging 2009;36(1):48–52.

57. Adams S, Baum R, Rink T, Schumm-Dräger PM, Usadel KH, Hör G. Limited value of fluorine-18 fluorodeoxyglucose positron emission tomography for the imaging of neuroendocrine tumours. Eur J Nucl Med 1998;25(1):79–83.

58. Eriksson B, Orlefors H, Oberg K, Sundin A, Bergström M, Långström B. Developments in PET for the detection of endocrine tumours. Best Pract Res Clin Endocrinol Metab 2005;19(2):311–324.

59. Bombardieri E, Maccauro M, De Deckere E, Savelli G, Chiti A. Nuclear medicine imaging of neuroendocrine tumours. Ann Oncol 2001;12(Suppl 2):S51–S61.

60. Anderson MA, Carpenter S, Thompson NW, Nostrant TT, Elta GH, Scheiman JM. Endoscopic ultrasound is highly accurate and directs management in patients with neuroendocrine tumors of the pancreas. Am J Gastroenterol 2000;95(9):2271–2277.

61. Gouya H, Vignaux O, Augui J, et al. CT, endoscopic sonography, and a combined protocol for preoperative evaluation of pancreatic insulinomas. AJR Am J Roentgenol 2003;181(4):987–992.

62. McAuley G, Delaney H, Colville J, et al. Multimodality preoperative imaging of pancreatic insulinomas. Clin Radiol 2005;60(10):1039–1050.

63. Scherübl H, Jensen RT, Cadiot G, Stölzel U, Klöppel G. Neuroendocrine tumors of the small bowels are on the rise: Early aspects and management. World J Gastrointest Endosc 2010;2(10):325–334.

64. Ardengh JC, de Paulo GA, Ferrari AP. EUS-guided FNA in the diagnosis of pancreatic neuroendocrine tumors before surgery. Gastrointest Endosc 2004;60(3):378–384.

65. Figueiredo FA, Giovannini M, Monges G, et al. EUS-FNA predicts 5-year survival in pancreatic endocrine tumors. Gastrointest Endosc 2009;70(5):907–914.

66. van Tuyl SA, van Noorden JT, Timmer R, Stolk MF, Kuipers EJ, Taal BG. Detection of small-bowel neuroendocrine tumors by video capsule endoscopy. Gastrointest Endosc 2006;64(1):66–72.

67. Khashab MA, Yong E, Lennon AM, et al. EUS is still superior to multidetector computerized tomography for detection of pancreatic neuroendocrine tumors. Gastrointest Endosc 2011;73(4):691–696.

68. Hruban RH, Klimstra DS, Pitman MB. Tumors of the pancreas. In: Atlas of tumor pathology. Washington, DC: Armed Forces Institute of Pathology, 2007; 23–376.

69. Alsohaibani F, Bigam D, Kneteman N, Shapiro AM, Sandha GS. The impact of preoperative endoscopic ultrasound on the surgical management of pancreatic neuroendocrine tumours. Can J Gastroenterol 2008;22(10):817–820.

70. Ginès A, Vazquez-Sequeiros E, Soria MT, Clain JE, Wiersema MJ. Usefulness of EUS-guided fine needle aspiration (EUS-FNA) in the diagnosis of functioning neuroendocrine tumors. Gastrointest Endosc 2002;56(2):291–296.

71. Palazzo L, Roseau G, Chaussade S, Salmeron M, Gaudric M, Paolaggi JA. Pancreatic endocrine tumors: contribution of ultrasound endoscopy in the diagnosis of localization [in French]. Ann Chir 1993;47(5):419–424.

72. Rappeport ED, Hansen CP, Kjaer A, Knigge U. Multidetector computed tomography and neuroendocrine pancreaticoduodenal tumors. Acta Radiol 2006;47(3):248–256.

73. Zimmer T, Stölzel U, Bäder M, et al. Endoscopic ultrasonography and somatostatin receptor scintigraphy in the preoperative localisation of insulinomas and gastrinomas. Gut 1996;39(4):562–568.

74. Lewis RB, Lattin GE Jr, Paal E. Pancreatic endocrine tumors: radiologic-clinicopathologic correlation. RadioGraphics 2010;30(6):1445–1464.

75. Low G, Panu A, Millo N, Leen E. Multimodality imaging of neoplastic and non-neoplastic solid lesions of the pancreas. RadioGraphics 2011;31(4):993–1015.

76. Bordeianou L, Vagefi PA, Sahani D, et al. Cystic pancreatic endocrine neoplasms: a distinct tumor type? J Am Coll Surg 2008;206(3):1154–1158.

77. Rha SE, Jung SE, Lee KH, Ku YM, Byun JY, Lee JM. CT and MR imaging findings of endocrine tumor of the pancreas according to WHO classification. Eur J Radiol 2007;62(3):371–377.

78. Han JH, Kim MH, Moon SH, et al. Clinical characteristics and malignant predictive factors of pancreatic neuroendocrine tumors [in Korean]. Korean J Gastroenterol 2009;53(2):98–105.

79. Haynes AB, Deshpande V, Ingkakul T, et al. Implications of incidentally discovered, nonfunctioning pancreatic endocrine tumors: short-term and long-term patient outcomes. Arch Surg 2011;146(5):534–538.

80. Vagefi PA, Razo O, Deshpande V, et al. Evolving patterns in the detection and outcomes of pancreatic neuroendocrine neoplasms: the Massachusetts General Hospital experience from 1977 to 2005. Arch Surg 2007;142(4):347–354.

81. Thoeni RF, Mueller-Lisse UG, Chan R, Do NK, Shyn PB. Detection of small, functional islet cell tumors in the pancreas: selection of MR imaging sequences for optimal sensitivity. Radiology 2000;214(2):483–490.

82. Anaye A, Mathieu A, Closset J, Bali MA, Metens T, Matos C. Successful preoperative localization of a small pancreatic insulinoma by diffusion-weighted MRI. JOP 2009;10(5):528–531.

83. Wang Y, Chen ZE, Yaghmai V, et al. Diffusion-weighted MR imaging in pancreatic endocrine tumors correlated with histopathologic characteristics. J Magn Reson Imaging 2011;33(5):1071–1079.

84. Hwang HS, Lee SS, Kim SC, Seo DW, Kim J. Intrapancreatic accessory spleen: clinicopathologic analysis of 12 cases. Pancreas 2011;40(6):956–965.

85. Sun HY, Kim SH, Kim MA, Lee JY, Han JK, Choi BI. CT imaging spectrum of pancreatic serous tumors: based on new pathologic classification. Eur J Radiol 2010;75(2):e45–e55.

86. Plöckinger U, Rindi G, Arnold R, et al. Guidelines for the diagnosis and treatment of neuroendocrine gastrointestinal tumours. A consensus statement on behalf of the European Neuroendocrine Tumour Society (ENETS). Neuroendocrinology 2004;80(6):394–424.

87. Wang SC, Parekh JR, Zuraek MB, et al. Identification of unknown primary tumors in patients with neuroendocrine liver metastases. Arch Surg 2010;145(3):276–280.

88. Levy AD, Sobin LH. From the archives of the AFIP: Gastrointestinal carcinoids: imaging features with clinicopathologic comparison. RadioGraphics 2007;27(1):237–257.

89. Bordi C. Gastric carcinoids. Ital J Gastroenterol Hepatol 1999;31(Suppl 2):S94–S97.

90. Rindi G, Azzoni C, La Rosa S, et al. ECL cell tumor and poorly differentiated endocrine carcinoma of the stomach: prognostic evaluation by pathological analysis. Gastroenterology 1999;116(3):532–542.

91. Levy AD, Taylor LD, Abbott RM, Sobin LH. Duodenal carcinoids: imaging features with clinical-pathologic comparison. Radiology 2005;237(3):967–972.

92. Hatzaras I, Palesty JA, Abir F, et al. Small-bowel tumors: epidemiologic and clinical characteristics of 1260 cases from the connecticut tumor registry. Arch Surg 2007;142(3):229–235.

93. Eriksson B, Klöppel G, Krenning E, et al. Consensus guidelines for the management of patients with digestive neuroendocrine tumors—well-differentiated jejunal-ileal tumor/carcinoma. Neuroendocrinology 2008;87(1):8–19.

94. Horton KM, Lawler LP, Fishman EK. CT findings in sclerosing mesenteritis (panniculitis): spectrum of disease. RadioGraphics 2003;23(6):1561–1567.

95. Masselli G, Polettini E, Casciani E, Bertini L, Vecchioli A, Gualdi G. Small-bowel neoplasms: prospective evaluation of MR enteroclysis. Radiology 2009;251(3):743–750.

96. Van Weyenberg SJ, Meijerink MR, Jacobs MA, et al. MR enteroclysis in the diagnosis of small-bowel neoplasms. Radiology 2010;254(3):765–773.

97. Bellutti M, Fry LC, Schmitt J, et al. Detection of neuroendocrine tumors of the small bowel by double balloon enteroscopy. Dig Dis Sci 2009;54(5):1050–1058.

98. Boudreaux JP, Klimstra DS, Hassan MM, et al. The NANETS consensus guideline for the diagnosis and management of neuroendocrine tumors: well-differentiated neuroendocrine tumors of the Jejunum, Ileum, Appendix, and Cecum. Pancreas 2010;39(6):753–766.

99. Pickhardt PJ, Levy AD, Rohrmann CA Jr, Kende AI. Primary neoplasms of the appendix: radiologic spectrum of disease with pathologic correlation. RadioGraphics 2003;23(3):645–662.

100. Shapiro R, Eldar S, Sadot E, Papa MZ, Zippel DB. Appendiceal carcinoid at a large tertiary center: pathologic findings and long-term follow-up evaluation. Am J Surg 2011;201(6):805–808.

101. Anthony LB, Strosberg JR, Klimstra DS, et al. The NANETS consensus guidelines for the diagnosis and management of gastrointestinal neuroendocrine tumors (nets): well-differentiated nets of the distal colon and rectum. Pancreas 2010;39(6):767–774.

102. Kobayashi K, Katsumata T, Yoshizawa S, et al. Indications of endoscopic polypectomy for rectal carcinoid tumors and clinical usefulness of endoscopic ultrasonography. Dis Colon Rectum 2005;48(2):285–291.

103. Fujishima H, Misawa T, Maruoka A, Yoshinaga M, Chijiiwa Y, Nawata H. Rectal carcinoid tumor: endoscopic ultrasonographic detection and endoscopic removal. Eur J Radiol 1993;16(3):198–200.

104. Prasad V, Ambrosini V, Hommann M, Hoersch D, Fanti S, Baum RP. Detection of unknown primary neuroendocrine tumours (CUP-NET) using (68)Ga-DOTA-NOC receptor PET/CT. Eur J Nucl Med Mol Imaging 2010;37(1):67–77.

105. Hauso O, Gustafsson BI, Kidd M, et al. Neuroendocrine tumor epidemiology: contrasting Norway and North America. Cancer 2008;113(10):2655–2664.

106. Jaffee IM, Rahmani M, Singhal MG, Younes M. Expression of the intestinal transcription factor CDX2 in carcinoid tumors is a marker of midgut origin. Arch Pathol Lab Med 2006;130(10):1522–1526.

107. Kuiper P, Verspaget HW, Overbeek LI, Biemond I, Lamers CB. An overview of the current diagnosis and recent developments in neuroendocrine tumours of the gastroenteropancreatic tract: the diagnostic approach. Neth J Med 2011;69(1):14–20.

108. Saqi A, Alexis D, Remotti F, Bhagat G. Usefulness of CDX2 and TTF-1 in differentiating gastrointestinal from pulmonary carcinoids. Am J Clin Pathol 2005;123(3):394–404.

109. Srivastava A, Hornick JL. Immunohistochemical staining for CDX-2, PDX-1, NESP-55, and TTF-1 can help distinguish gastrointestinal carcinoid tumors from pancreatic endocrine and pulmonary carcinoid tumors. Am J Surg Pathol 2009;33(4):626–632.

110. Johanssen S, Boivin M, Lochs H, Voderholzer W. The yield of wireless capsule endoscopy in the detection of neuroendocrine tumors in comparison with CT enteroclysis. Gastrointest Endosc 2006;63(4):660–665.

111. Boudreaux JP, Putty B, Frey DJ, et al. Surgical treatment of advanced-stage carcinoid tumors: lessons learned. Ann Surg 2005;241(6):839–845; discussion 845–846.

112. Elsayes KM, Menias CO, Bowerson M, Osman OM, Alkharouby AM, Hillen TJ. Imaging of carcinoid tumors: spectrum of findings with pathologic and clinical correlation. J Comput Assist Tomogr 2011;35(1):72–80.

113. Gutierrez G, Daniels IR, Garcia A, Ramia JM. Peritoneal carcinomatosis from a small bowel carcinoid tumour. World J Surg Oncol 2006;4:75.

114. Hlatky R, Suki D, Sawaya R. Carcinoid metastasis to the brain. Cancer 2004;101(11):2605–2613.

115. Meijer WG, van der Veer E, Jager PL, et al. Bone metastases in carcinoid tumors: clinical features, imaging characteristics, and markers of bone metabolism. J Nucl Med 2003;44(2):184–191.

116. Fenwick SW, Wyatt JI, Toogood GJ, Lodge JP. Hepatic resection and transplantation for primary carcinoid tumors of the liver. Ann Surg 2004;239(2):210–219.

117. Schillaci O, Spanu A, Scopinaro F, et al. Somatostatin receptor scintigraphy in liver metastasis detection from gastroenteropancreatic neuroendocrine tumors. J Nucl Med 2003;44(3):359–368.

118. Dromain C, de Baere T, Lumbroso J, et al. Detection of liver metastases from endocrine tumors: a prospective comparison of somatostatin receptor scintigraphy, computed tomography, and magnetic resonance imaging. J Clin Oncol 2005;23(1):70–78.

119. Elias D, Lefevre JH, Duvillard P, et al. Hepatic metastases from neuroendocrine tumors with a "thin slice" pathological examination: they are many more than you think. Ann Surg 2010;251(2):307–310.

120. Gibril F, Jensen RT. Diagnostic uses of radiolabelled somatostatin receptor analogues in gastroenteropancreatic endocrine tumours. Dig Liver Dis 2004;36(Suppl 1):S106–S120.

121. Dromain C, de Baere T, Baudin E, et al. MR imaging of hepatic metastases caused by neuroendocrine tumors: comparing four techniques. AJR Am J Roentgenol 2003;180(1):121–128.

122. Bruegel M, Holzapfel K, Gaa J, et al. Characterization of focal liver lesions by ADC measurements using a respiratory triggered diffusion-weighted single-shot echoplanar MR imaging technique. Eur Radiol 2008;18(3):477–485.

123. Koh DM, Brown G, Riddell AM, et al. Detection of colorectal hepatic metastases using MnDPDP MR imaging and diffusion-weighted imaging (DWI) alone and in combination. Eur Radiol 2008;18(5):903–910.

124. Vossen JA, Buijs M, Liapi E, Eng J, Bluemke DA, Kamel IR. Receiver operating characteristic analysis of diffusion-weighted magnetic resonance imaging in differentiating hepatic hemangioma from other hypervascular liver lesions. J Comput Assist Tomogr 2008;32(5):750–756.

125. Chiti A, van Graafeiland BJ, Savelli G, et al. Imaging of neuroendocrine gastro-enteropancreatic tumours using radiolabelled somatostatin analogues. Ital J Gastroenterol Hepatol 1999;31(Suppl 2):S190–S194.

126. Ambrosini V, Campana D, Bodei L, et al. 68Ga-DOTANOC PET/CT clinical impact in patients with neuroendocrine tumors. J Nucl Med 2010;51(5):669–673.

127. Gabriel M, Decristoforo C, Kendler D, et al. 68Ga-DOTA-Tyr3-octreotide PET in neuroendocrine tumors: comparison with somatostatin receptor scintigraphy and CT. J Nucl Med 2007;48(4):508–518.

128. Diederichs CG, Staib L, Vogel J, et al. Values and limitations of 18F-fluorodeoxyglucose-positron-emission tomography with preoperative evaluation of patients with pancreatic masses. Pancreas 2000;20(2):109–116.

129. Gould MK, Kuschner WG, Rydzak CE, et al. Test performance of positron emission tomography and computed tomography for mediastinal staging in patients with non-small-cell lung cancer: a meta-analysis. Ann Intern Med 2003;139(11):879–892.

130. Putzer D, Gabriel M, Henninger B, et al. Bone metastases in patients with neuroendocrine tumor: 68Ga-DOTA-Tyr3-octreotide PET in comparison to CT and bone scintigraphy. J Nucl Med 2009;50(8):1214–1221.

131. Ruszniewski P, Delle Fave G, Cadiot G, et al. Well-differentiated gastric tumors/carcinomas. Neuroendocrinology 2006;84(3):158–164.

132. Kasono K, Hyodo T, Suminaga Y, et al. Contrast-enhanced endoscopic ultrasonography improves the preoperative localization of insulinomas. Endocr J 2002;49(4):517–522.

133. Harring TR, Nguyen NT, Goss JA, O'Mahony CA. Treatment of liver metastases in patients with neuroendocrine tumors: a comprehensive review. Int J Hepatol 2011;2011:154541.

134. Kianmanesh R, Sauvanet A, Hentic O, et al. Two-step surgery for synchronous bilobar liver metastases from digestive endocrine tumors: a safe approach for radical resection. Ann Surg 2008;247(4):659–665.

135. Mazzaferro V, Pulvirenti A, Coppa J. Neuroendocrine tumors metastatic to the liver: how to select patients for liver transplantation? J Hepatol 2007;47(4):460–466.

136. Basu B, Sirohi B, Corrie P. Systemic therapy for neuroendocrine tumours of gastroenteropancreatic origin. Endocr Relat Cancer 2010;17(1):R75–R90.

137. Pitt SC, Knuth J, Keily JM, et al. Hepatic neuroendocrine metastases: chemo- or bland embolization? J Gastrointest Surg 2008;12(11):1951–1960.

138. Lawrence B, Gustafsson BI, Kidd M, Modlin I. New pharmacologic therapies for gastroenteropancreatic neuroendocrine tumors. Gastroenterol Clin North Am 2010;39(3):615–628.

139. Krenning EP, Valkema R, Kwekkeboom DJ, et al. Molecular imaging as in vivo molecular pathology for gastroenteropancreatic neuroendocrine tumors: implications for follow-up after therapy. J Nucl Med 2005;46(Suppl 1):76S–82S.

140. Jamar F, Fiasse R, Leners N, Pauwels S. Somatostatin receptor imaging with indium-111-pentetreotide in gastroenteropancreatic neuroendocrine tumors: safety, efficacy and impact on patient management. J Nucl Med 1995;36(4):542–549.

141. Lebtahi R, Cadiot G, Sarda L, et al. Clinical impact of somatostatin receptor scintigraphy in the management of patients with neuroendocrine gastroenteropancreatic tumors. J Nucl Med 1997;38(6):853–858.

142. Ducreux M, Ruszniewski P, Chayvialle JA, et al. The antitumoral effect of the long-acting somatostatin analog lanreotide in neuroendocrine tumors. Am J Gastroenterol 2000;95(11):3276–3281.

143. Gonzalez MA, Biswas S, Clifton L, Corrie PG. Treatment of neuroendocrine tumours with infusional 5-fluorouracil, folinic acid and streptozocin. Br J Cancer 2003;89(3):455–456.

144. Raymond E, Dahan L, Raoul JL, et al. Sunitinib malate for the treatment of pancreatic neuroendocrine tumors. N Engl J Med 2011;364(6):501–513.

145. Yao JC, Shah MH, Ito T, et al. Everolimus for advanced pancreatic neuroendocrine tumors. N Engl J Med 2011;364(6):514–523.

146. Arnold R, Chen YJ, Costa F, et al. ENETS Consensus Guidelines for the Standards of Care in Neuroendocrine Tumors: follow-up and documentation. Neuroendocrinology 2009;90(2):227–233.

147. Liapi E, Geschwind JF, Vossen JA, et al. Functional MRI evaluation of tumor response in patients with neuroendocrine hepatic metastasis treated with transcatheter arterial chemoembolization. AJR Am J Roentgenol 2008;190(1):67–73.

148. Barbe C, Murat A, Dupas B, et al. Magnetic resonance imaging versus endoscopic ultrasonography for the detection of pancreatic tumours in multiple endocrine neoplasia type 1. Dig Liver Dis 2012;44(3):228–234.

149. Ferner RE, Huson SM, Thomas N, et al. Guidelines for the diagnosis and management of individuals with neurofibromatosis 1. J Med Genet 2007;44(2):81–88.